SYNTHESIS OF HYDROXYAPATITE FROM FISH BONE (SCOMBER SCOMBRUS) USING THERMAL DECOMPOSITION METHOD

SUGUNA A/P JEGANATHAN

FACULTY OF ENGINEERING
UNIVERSITY OF MALAYA
KUALA LUMPUR

2018

SYNTHESIS OF HYDROXYAPATITE FROM FISH BONE (SCOMBER SCOMBRUS) USING THERMAL DECOMPOSITION METHOD

SUGUNA A/P JEGANATHAN

RESEARCH REPORT SUBMITTED IN PARTIAL FULFILMENT OF THE REQUIREMENTS FOR THE DEGREE OF MASTER OF ENGINEERING

FACULTY OF ENGINEERING
UNIVERSITY OF MALAYA
KUALA LUMPUR

2018

UNIVERSITY OF MALAYA
ORIGINAL LITERARY WORK DECLARATION

Name of Candidate: Suguna A/P Jeganathan

Matric No: KQG160009

Name of Degree: Master of Engineering (Manufacturing)

Title of Project Paper/Research Report/Dissertation/Thesis ("this Work"): Synthesis of Hydroxyapatite from Fish Bone (Scomber Scombrus) Using Thermal Decomposition Method

Field of Study: Bio-Ceramic

I do solemnly and sincerely declare that:

(1) I am the sole author/writer of this Work;
(2) This Work is original;
(3) Any use of any work in which copyright exists was done by way of fair dealing and for permitted purposes and any excerpt or extract from, or reference to or reproduction of any copyright work has been disclosed expressly and sufficiently and the title of the Work and its authorship have been acknowledged in this Work;
(4) I do not have any actual knowledge nor do I ought reasonably to know that the making of this work constitutes an infringement of any copyright work;
(5) I hereby assign all and every rights in the copyright to this Work to the University of Malaya ("UM"), who henceforth shall be owner of the copyright in this Work and that any reproduction or use in any form or by any means whatsoever is prohibited without the written consent of UM having been first had and obtained;
(6) I am fully aware that if in the course of making this Work I have infringed any copyright whether intentionally or otherwise, I may be subject to legal action or any other action as may be determined by UM.

Candidate's Signature Date:

Subscribed and solemnly declared before,

Witness's Signature Date:

Name:

Designation:

SYNTHESIS OF HYDROXYAPATITE FROM FISH BONE (SCOMBER SCOMBRUS) USING THERMAL DECOMPOSITION METHOD

ABSTRACT

There are numerous methods that can be used to synthesise HAp using various costly precursors. Studies related to fish bone derived hydroxyapatite are very limited and are usually focused on the synthesis parameters rather than mechanical property evaluation. Therefore, the present study is aimed to develop a process to synthesize HAp from fish bones and to evaluate the mechanical properties of the derived HAp.

Various calcination temperatures were studied to determine the optimum temperature to produce high purity HAp. As-synthesized HAp powder was evaluated in term of mechanical properties and morphology. The sinterability of compacted HAp powder was investigated between 800°C to 1200°C.

The study found that synthesized HAp powder looked a needle-like shape, similar to that observed in the human bones. Sintered HAp was stable up 1000°C temperature, whereas beyond this point, HAp began to decompose to its secondary phase (α-TCP and β-TCP). A near density of 98% was achieved at 1000°C, thus the density start to decrease beyond to this temperature due to the decomposition of Hap to TCP. This can correlated with SEM images which showed in prominent pore isolation when increased sintering temperature resulted forming a less dense ceramic. HAp samples showed the highest hardness of 3.49 GPa at 1000°C. The Vickers hardness of sintered HAp was increase as the relative density increase.

Keywords: Hydroxyapatite, Thermal Calcination, Mechanical properties, Fish bone

SINTESIS HYDROXYAPATITE DARIPADA TULANG IKAN (SCOMBRUS SCOMBRUS) MENGGUNAKAN KEADAH THERMAL DECOMPOSITION

ABSTRAK

Terdapat banyak kaedah yang boleh digunakan untuk sintesis HAp menggunakan pelbagai jenis prekursor yang mahal. Kajian yang berkaitan dengan HAp yang diperolehi daripada tulang ikan sangat terhad dan biasanya tertumpu pada parameter sintesis daripada penilaian ciri-ciri mekanikal. Oleh itu, kajian ini bertujuan untuk mencadangkan sebuah proses sintesis HAp dari tulang ikan dan untuk menilai sifat-sifat mekanikal HAp yang diperolehi.

Kaedah Thermal Calcination (TC) yang ringkas dan murah digunakan dalam kajian ini untuk mensintesis HAp yang diperolehi daripada tulang ikan. Pelbagai suhu telah dikaji untuk menentukan suhu optimum untuk menghasilkan ketulenan HAp yang tinggi. As-sintetik HAp telah dinilai dari segi sifat mekanik dan morfologinya. HAp diselidiki antara 800°C hingga 1200°C.

Kajian mendapati bahawa serbuk HAp yang disintesis menunjukkan morfologi seperti jarum, sama seperti yang diperhatikan dalam tulang manusia. HAp stabil sehingga suhu tinggi 1000°, sedangkan di luar titik ini, HAp mula mengurai ke fasa sekunder (α-TCP dan β-TCP). Ketumpatan hampir 98% dicapai pada 1000°C. Ini bersamaan dengan imej SEM yang menunjukkan bahawa peningkatan suhu sintering mengakibatkan pengasingan liang yang menonjol, sehingga membentuk seramik yang kurang padat. Sampel HAp mempamerkan kekerasan Vickers tertinggi sehingga 3.49 GPa pada suhu1000°C. Kekerasan HAp diperhatikan dikawal oleh ketumpatan relatif.

Kata kunci: Hydroxyapatite, Thermal Calcination, Ciri-ciri mekanik, Tulang ikan

ACKNOWLEDGEMENT

First and foremost, I would like to express my utmost gratitude to my project supervisor, Prof. Dr. Hendrik Simon Cornelis Metselaar for providing me with the opportunity to purse my postgraduate studies at university of Malaya. Not only have they provided me with insightful ideas and valuable advice, they have also been the source of motivation throughout my duration in university of Malaya as a postgraduate student. I would also like to take this opportunity to thank:

- Mr Amir Reza Akhiani**,** postgraduate student to help me throughout my research and guide me until complete this project.
- Mr tauqik, Lab Assistant at ceramic lab to guide me on the procedure for certain experiments.

I also dedicate my dissertation work to my family. A special feeling of gratitude to my late loving mother, Vijayakumari Munusamy. I hope that this achievement will complete the dream that you had for me all those many years ago when you chose to give me the best education you could.

TABLE OF CONTENTS

LIST OF FIGURES

LIST OF TABLE

LIST OF SYMBOLS AND ABBREVIATIONS

SEM: Scanning Electron Microscope

EDX: Energy-Dispersive X-ray spectroscopy

FTIR: Fourier-Transform Infrared spectroscopy

HAp: Hydroxyapatite

TGA: Thermogravimetric Analysis

CaP: Calcium Phosphate

TCP: Tricalcium Phosphate

DTG: Derivative Thermogravimetry

DTA: Differential Thermal Analysis

XRD: X-ray Diffraction Analysis

CHAPTER 1: INTRODUCTION

1. Introduction

The primary function of bone is to maintaining the shape of the body, in locomotion, protecting the soft tissues and supplying the work frame for bone marrow. A lifetime execution of these support functions depends on a healthy skeleton, continue remodelling in which old bone is tarnished by the bone-resorbing cells, osteoclasts, and then replaced by new bone tissue formed by the bone-forming cells, osteoblasts. This remodelling process requires a physical interaction of bone with these bone cells. Bone is consists of roughly 65% of mineral and 35% of organic by mass. The mineral phase is hydroxyapatite ($Ca_{10}(PO_4)_6(OH)_2$) (HAp) and organic phase that are B90% type I collagen, B5% non-collagenous proteins (NCPs), B2% lipids by weight). Therefore HAp plays a vital role in the bone replacement or regeneration of bone tissues. Due to the limited supply of natural bone for bone replacement, the need for synthetic bone to substitutes which possess the same physiochemical and biological properties as natural bone is ever increasing. This has created an importance in the development of artificial materials as bone graft substitutes. The HAp is not only a biocompatible, non-toxic, non-immunogenic agent, non-inflammatory, but also bioactive. HAp can directly bond to the host bone as artificial teeth or bones. It is widely used in orthopaedic applications nowadays.

There are two manufacturing methods of hydroxyapatite (HAp) which are by extraction from natural sources or chemical synthesis. Chemical synthesis is concerned with different methods have been applied like precipitation method from salts solutions, wet mechanical chemical route with $Ca(OH)_2$ and $(NH_4)_2HPO_4$ as precursors, a sol–gel method by applying phosphor alkoxide and Ca nitrate, solid-state reaction process with $Ca(OH)_2$ and CaHPO4 as starting materials. Source of natural calcium also can obtain from egg-shells, coral and sea-shells. For extracted HAp from the natural bones there are three techniques like calcination of bone, bone treatment at elevated temperatures with sodium hydroxide solution, and bone treatment under hydrothermal conditions. Hydroxyapatite of natural origin contain different Ca/P ratio compared to the synthetic one. It contains carbonate group traces of metal like magnesium and sodium mixtures (Brzezi, Haberko, Sitarz, Bu, & Macherzy, 2015).

Scope and objective of the research:

The sintered bone from biogenic source such as from biowaste which include fish bones, corals, bovine bones, eggshells and others are biomaterial that contains natural calcium phosphate compounds, is perceived to be better accepted by the living tissues because of its physiochemical similarity to the human bone. Sintered fish bone is made of hydroxyapatite (HAp), which is the most stable phase of calcium phosphate apatite that has demonstrated excellent biocompatibility and bioactivity with hard tissues. The scope of the research is to extract the pure HAp from the fish bone and do characteristic tests like FTIR, TGA, SEM, Microvicker's hardness and XRD for better understanding of the HAp synthesis from the fish bone.

Objective of this study:

1) To extract the pure HAp from the fish bone with a Ca/P ratio close to 1.67
2) To study the morphology of the HAp extracted from the fish
3) To study the chemical composition of the pure HAp
4) To study the effect of calcination temperature on the HAp physical and mechanical properties.

Outline of the thesis:

This thesis is divided into five chapters. Chapter 1 presents of a brief overview about biomaterials, identifying the gaps in the literature and establishing the objective of this research. The literature review is presented in chapter 2. This chapter deliberates on the findings in the available literatures on the concept of HAp bioceramic and strategies that have been employed for it’s used as a presented in chapter 3. The results obtained in this research and discussions are presented in chapter in chapter 4. In this chapter, the effect of sintering temperature on the thermal stability of HAp derived from fish bone as well as its mechanical properties are discussed. The resulting in microstructure of the fish bone HAp as a function of sintering temperature is also deliberated. Finally, the conclusion draw from the present research is presented in chapter 5.

CHAPTER 2: LITERATURE REVIEW

2 Literature Review

2.1 Bone

Bones are a support system that consists of hydroxyapatite (HAp), Collagen and water. HAp amounts 65% of bones, while 20% of collagen and water is around 15% (Szcze, Ho, & Chibowski, 2017). With number of tragedy or trauma and inherent bone disability by birth/age/disease, the needs and requirements for artificial bone substitutes have been increasing over time. The need for bone in the fields of dental, cranial, maxillofacial, orthopaedic and applications for spinal has increase significantly over the time (Markovic, Lukic, & Bracko, 2014). Transplantation or implantation method are used to replace the bones. The transplantation method can be autografting or allografting. An autograft is a bone taken from another part of the patient’s own body and transplanted while an allograft is defined as bone that been harvested from one individual and implanted into another different individual (Markovic et al., 2014). However, this method can be risky due to price, size of grafts, potentially damage of donor tissues, grafts availability and bacterial infections such as HIV and others. Other than this, implantation synthetic materials can use which are easily available, reliable and reproducible. Amongst the synthetic materials, the hydroxyapatite (HAp) which is bio ceramic having a same chemical formula of $Ca_{10}(PO_4)_6(OH)_2$ compatible well with the mineral component of human bone tissues (Ramesh et al., 2013).

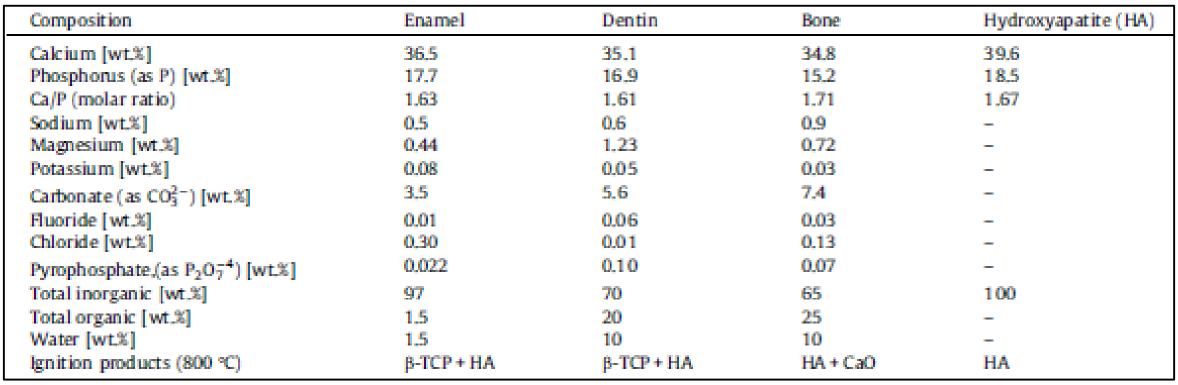

Composition	Enamel	Dentin	Bone	Hydroxyapatite (HA)
Calcium [wt.%]	36.5	35.1	34.8	39.6
Phosphorus (as P) [wt.%]	17.7	16.9	15.2	18.5
Ca/P (molar ratio)	1.63	1.61	1.71	1.67
Sodium [wt.%]	0.5	0.6	0.9	–
Magnesium [wt.%]	0.44	1.23	0.72	–
Potassium [wt.%]	0.08	0.05	0.03	–
Carbonate (as CO_3^{2-}) [wt.%]	3.5	5.6	7.4	–
Fluoride [wt.%]	0.01	0.06	0.03	–
Chloride [wt.%]	0.30	0.01	0.13	–
Pyrophosphate (as $P_2O_7^{-4}$) [wt.%]	0.022	0.10	0.07	–
Total inorganic [wt.%]	97	70	65	100
Total organic [wt.%]	1.5	20	25	–
Water [wt.%]	1.5	10	10	–
Ignition products (800 °C)	β-TCP + HA	β-TCP + HA	HA + CaO	HA

Figure 2-1: Bone compositions

Source: (Bose & Tarafder, 2012)

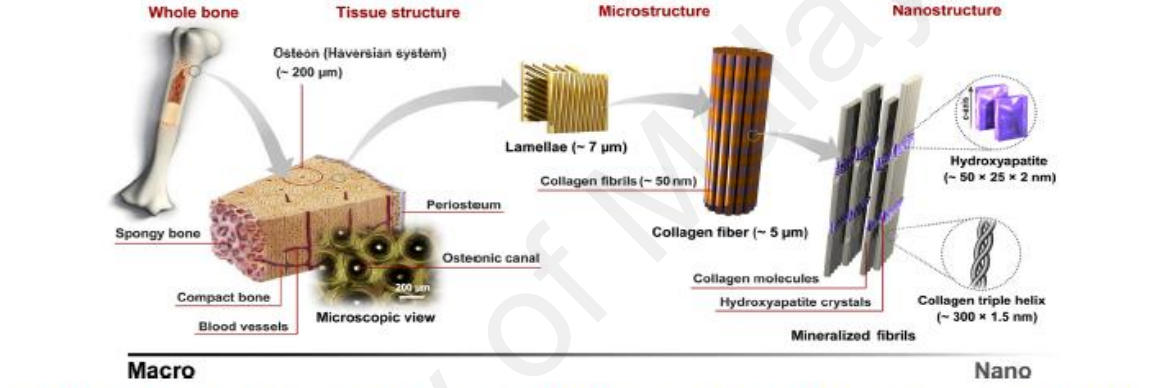

Fig. 1. The hierarchical structure of typical bone at various length scales. The microstructure of cortical or compact bone consists of Haversian systems (circles in cross-section and microscopic view) with osteonic canals and lamellae, and at the nanoscale, the structural framework is collagen fibers composed of bundles of mineralized collagen fibrils.

Figure 2-2: Bone structure

Source: (Sadat-shojai, Khorasani, Dinpanah-khoshdargi, & Jamshidi, 2013)

The skeleton contains two main structural bone type know as cortical bone and the trabecular bone. The cortical bone is dense with a low surface area and forms around the marrow cavity to protect it. Trabecular or also called as spongy bone has characterise of low density with a larger surface area compared to cortical bone. Long bones, flat bones and vertebrae is filed by trabecular one at the centre and consists of an interconnecting meshwork of bony trabecular, separated by spaces that are filled with bone marrow. The whole support system consist around 80% of cortical bone and the distribution of the cortical and trabecular bone will be different at different parts of body. (Ralston, 2013). Cortical bone is stiffer and only can withstand the strains aroun 2% while trabecular bone can withstand higher strains up to 30%. This variability to the largest part depends on the trabecular bone’s apparent density. Due to its heterogeneity, the apparent density and thus the trabecular bone modulus can vary 100- fold from one location to another within the same metaphysis (Osterhoff, 2016).

2.2 Calcium Phosphate

Bone and tooth are consists of majority calcium phosphate salts. Among the CaP salts, hydroxyapatite ($Ca_{10}(PO_4)_6(OH)_2$,HAp), as the thermodynamically most stable crystalline phase of CaP in body fluid, possesses the most similarity to the mineral part of bone (Sadat-shojai et al., 2013). CaPs can exist in different phases based on different of temperature, impurities, and the presence of water. Generally all CaP salts different in bioactivity, and also degradation rate. Bioactivity and degradation behaviour generally depend on the Ca/P ratio, crystallinity and phase purity. Monocalcium phosphate (MCP) is the anhydrous form of monocalcium phosphate monohydrate (MCPM). Due to high solubility and acidity properties, both MCP and MCPM are not biocompatible. Precipitated hydroxyapatite (PHA) sometimes called bioactive calcium-deficient hydroxyapatite (CDHA), have a complex chemical structure. The Ca/P ratio of CDHA is around between 1.50 and 1.67. Bone mineral is similar to CDHA except in the presence of carbonate (CO_2^{3-}) and trace elements, for instance, K^+, Na^+, Sr^{2+}, Mg^{2+}, Zn^{2+}. Amorphous calcium phosphate (ACP) is same like CDHA, while tetracalcium phosphate (TTCP) and octacalcium phosphate (OCP) can be withstand at a higher temperature than other CaPs. HAp and β-TCP are the most commonly used CaP because of their biocompatibility and osteogenic property. Β-TCP is known as bio-resorbable ceramic due to its higher solubility characteristic than HAp. development of biphasic calcium phosphate (BCP)-based biomaterials which are mixture of HAp and β-TCP in order to control the solubility characteristic of β-TCP (Bose & Tarafder, 2012).

2.3 Hydroxyapatite

Hydroxyapatite [$Ca_{10}(PO_4)_6(OH)_2$] is a bio-ceramic which is porous and granulated in nature and has big impact in the in biomedical, dentistry and orthopaedics. Hydroxyapatite is not only biocompatible and non-toxic but also a non-inflammatory and even non immunogenic agent, and also bioactive. Hydroxyapatite has got the ability to form a direct chemical bond with living tissues (Mehta & George, 2014) . Hydroxyapatite has been extensively study to create artificial bone grafts made from HAp, as a metal surface coating by HAp or as vehicle for drug delivery.

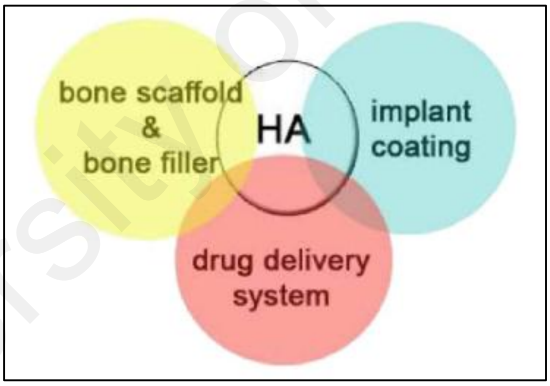

Figure 2-3: Uses of Hap

Source:(Szcze et al., 2017)

Beside the bone grafting, the HAp can also act as a coating for the synthesis bone especially metal based grafting. Mostly the implants materials are made of titanium alloys due to their strength like mechanical properties, endurance, low weight and chemical inertness in body fluids. Metallic bone grafting implants have better hardness and mechanical properties but poor biocompatibility and osseointegration. To improve the compatibility properties of metals the HAp is extensively studied as a coating on the metal grafting. (Szcze et al., 2017). HAp coatings on the metal surface can be made by many ways like plasma spraying, electrophoretic deposition, pulsed laser deposition, sol-gel deposition, spin-coating, sputtering techniques, ion beam assisted deposition, and many other techniques. The parameter control during coating processes is vital for make sure good biocompatible coatings. HAp bioceramics are brittle. Furthermore, an increase in amorphous phase, micro-porosity and grain size will the decrease the mechanical properties significantly. In addition, high crystallinity, high fracture toughness and better compressive and tensile strength if the HAp have low porosity percentage and small grain size. Due to the poor mechanical properties of HAp unable use widely as a load-bearing function. The HAp bioceramics has lower fracture toughness which is does not exceed ~1.2 MPa·m$^{1/2}$ compared to natural human bone is around 2–12 MPa·m$^{1/2}$. Tensile strengths, bending and compressive of dense HAp are in the range of 38–300 MPa, 38–250 MPa and 120–900 MPa respectively, whereas those values for the porous HAp are ~3 MPa, 2–11 MPa and 2–100 MPa respectively. The strength was found to increase as the Ca/P ratio increasing, and will decreasing back after reach the optimum Ca/P. Furthermore, the strength of the HAp also influence by the pore geometry, (Prakasam, 2015).

2.4 Synthesis Method

There are many methods to prepare HAp through chemical and biogenic extraction like dry method, wet method and biogenic extraction. The different methods of the synthesis will produce different properties of HAp. The chemical agent, the parameters and synthesis route are importance to produce the Hap with precise properties (Anitha &

Pandya, 2014). Generally we looking for the nano-sized HAp due to its uses in the medical application (Abidi & Murtaza, 2014).

2.4.1. Solid-state

Solid-state reaction a as dry methods, a relatively simple and low cost process, that can be employed in the mass production of HAp powder. In a typical procedure, precursors of calcium and phosphate are first milled and then calcined at a very high temperature from 1000-1250 °C. However, the HAp produce was irregular in shape and micrometer sized grains (Pramanik, 2007). Other than, solid stated synthesis, the mechanochemical method is also widely used in the synthesis of HAp to overcome the limitation in the solid state. Recently, it has been demonstrated that mechanochemically induced solid-state reactions can also be used for the production of nanoparticles. Mechanochemical processing works through repeated welding, deformation and fracture of the mixture of reactants. The high temperature during solid-state displacement reactions leads to micrometer-sized particles, whilst the reactions that occur in a steady state manner in mechanochemical synthesis result in a nanoscale mixture of HAp phases (Tsuzuki, 2003). Based on Sharifah Adzila et al. the high rotation speed of ball milling will increase the crystallinity and crystallite size of the obtained powders. However, the high speed will reduces the particle size of HA powder as well as the agglomeration of particles. Prolonged milling time does not result in changes of the powder properties. Thus, the present mechanochemical synthesis route from dry mixing condition may be a potential route to produce HAp nanopowder for biomedical implant application (Adzila, Sopyan, & Hamdi, 2011).

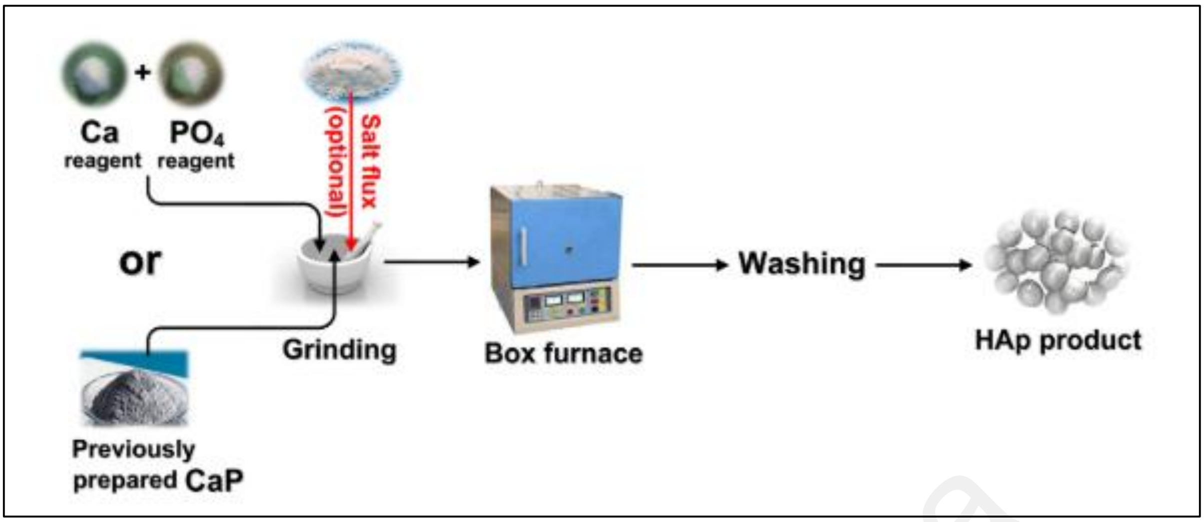

Figure 2-4: Preparation of HAp powder using solid-state method

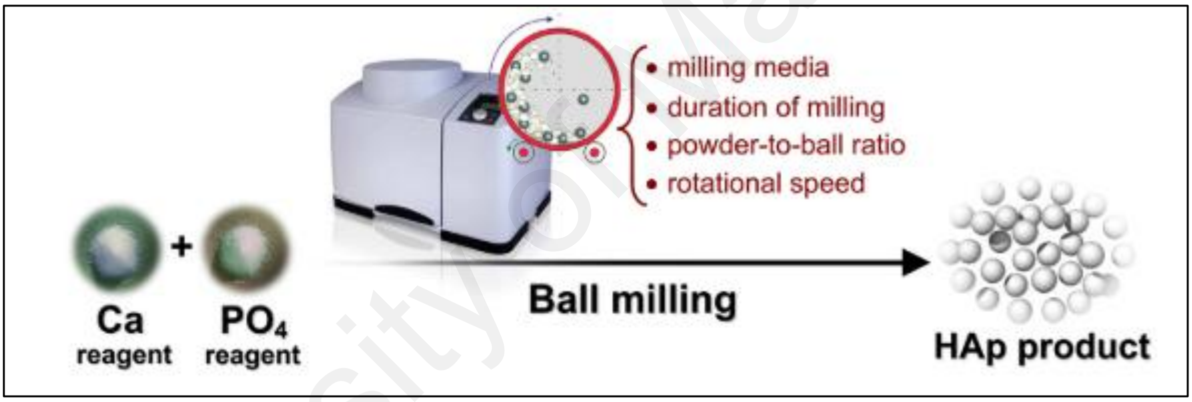

Figure 2-5: Preparation of HAp using mechanochemical method

Source:(Sadat-shojai et al., 2013)

2.4.2 Precipitation

Precipitation is one of the most popular and widely researched techniques for the synthesis of HAp. This technique is also known as wet precipitation or chemical precipitation or aqueous precipitation and chosen widely to synthesize HAp due to the high yield amount of HAp that can be produced by precipitation technique (Nayak, 2010). The chemical precursors can be orthophosphoric acid, calcium hydroxide, ammonium phosphate, calcium hydrogen phosphate and others. Some of the possible chemical reaction to form HAp by precipitation are:

$10\ Ca(OH)_2 + 6\ H_3PO_4 \rightarrow Ca_{10}(PO_4)_6(OH)_2 + 18\ H_2O$……………………………(1)

$10\ Ca(OH)_2 + 6\ (NH_4)_2.HPO_4 \rightarrow Ca_{10}(PO_4)6(OH)_2 + 6\ H_2O + 12\ NH_4OH$ ……….(2)

$7\ Ca(OH)_2 + 3\ Ca(H_2PO_4)2.H_2O \rightarrow Ca_{10}(PO_4)_6(OH)_2 + 15\ H_2O$ ………………….(3)

When the amount of reagents exceeds the solubility limit then the solution is called supersaturated. Crystal growth and nucleation occur once the solution is supersaturated and this is brought about by filtrating phosphate solution into the calcium solution forming a suspension of precipitated particles. The main parameters in the precipitation synthesis route are solution pH, concentration, and temperature. Thus these reaction parameters must be controlled in order to generate a homogeneous product (Cox, 2014). The reaction temperature, stirring time and reaction pH effect on the HAp were discussed by manoj et al in their paper. The pH of 11.5 required for HAp prepared at room temperature with 48 h stirring to show a well- defined size and morphology, better than the HAp nanostructures prepared under other conditions. Furthermore, the phase changed from HAp to β-TCP and the morphology changed from particles to nanorods after increase the reaction temperature to 90°C. The results obtained from their studies shows that the physicochemical nature of the HAp strongly based on the reaction parameters (Manoj et al., 2015).

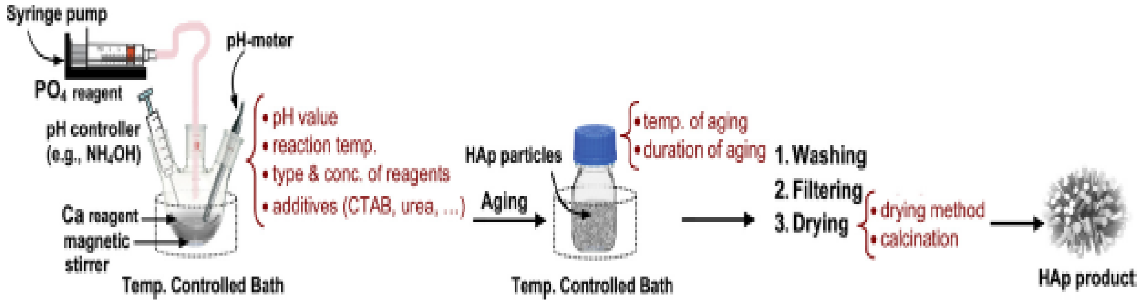

Fig. 6. Preparation of HAp nanoparticles via conventional chemical precipitation.

Figure 2-6: Preparation of HAp using conventional chemical precipitation

Source:(Sadat-shojai et al., 2013)

2.4.3 Hydrothermal

The hydrothermal conversion methods generally take place at high temperature around of 150˚C to 300˚C and high pressure. This hydrothermal method is a modification of the precipitation method, as in the hydrothermal method the temperature and the pressure to increase the reaction rate. Usually, stability of reaction product is more important. Precipitated in a fast process anyway. The main chemicals are calcium, phosphate, and alkaline sources to control the Ca/P ratio of the products by pH and the desired shape. Many regulating agents are used to prepare different morphology of HAp structures (Qi et al., 2015). Normally two parameters are used to control the shape of the HAp which are the regulating agents types and the pH of the processes.

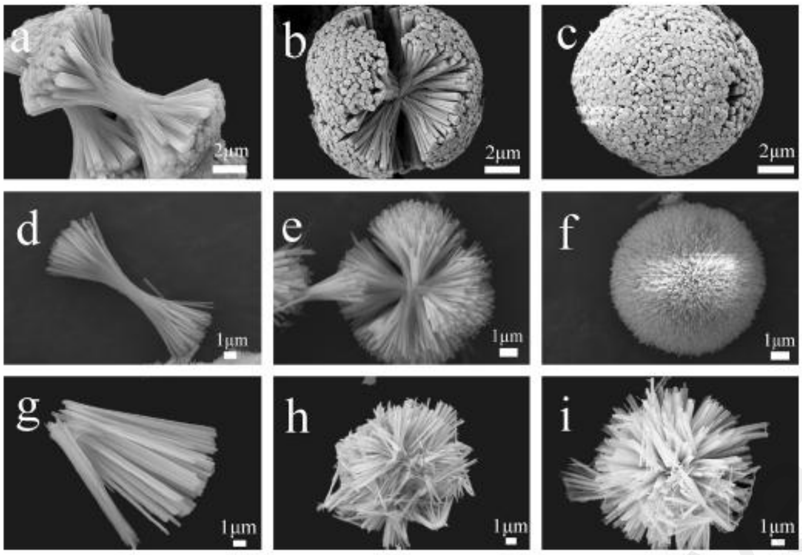

Figure 2-7: Morphology of the different pH control

Source: (Qi et al., 2015)

2.4.4 Sol-Gel

Sol–gel is a method to form a nano particle to microstructure size of HAp with crystalline structure. Based on the vitro and in vivo observations, the crystal structure are very efficient to improve the contact and stability at the artificial/natural interface (Bakan, 2013). The advantages of sol–gel synthesis of HAp include:

(a) Carrying out the reaction at room temperature

(b) Obtaining the gel formation without any dispersant and

(c) Forming nano sized HAp without using any grinding process.

In sol gel the phosphorus and calcium are most commonly precursors. The selected calcium precursor which is normally calcium nitrate, will dissolved in ethanol and then added drop wise into hydrolysed phosphorus in sol gel method. The mixed solution is then refluxed at the desired temperature and solvents are evaporated until achieve a sol–gel. Chemical nature of the precursors important to form apatite phase based on chemical activity and the temperature required. The sol–gel route, as shown in Figure 2-8, consists of producing a CaP precursors in homogeneous solution that can be mixed with the reagent or water. Secondly, the solution is changed to a 'gel' by condensation. Subsequently, sol–gel slurry undergoes dehydration process through calcination processes. Sol–gel method is known as cost-effective and simple preparation, besides having the ability to form complex shapes, similar to biomimetic coatings (Hassan, 2016). However in a recent study, the sol gel method was made 50 times quicker by using a rotary evaporator to dry the slurry without aging with only in 1 hour (Ben-Arfa, 2017).

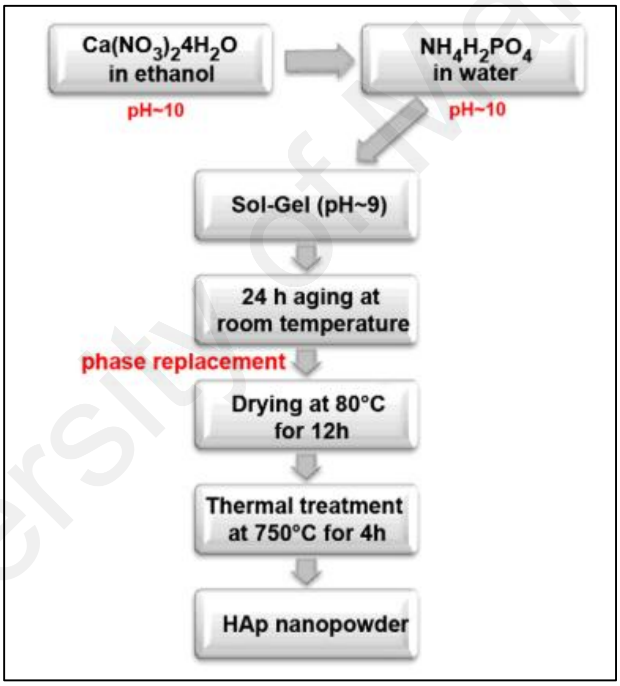

Figure 2-8: Route synthesis of the sol gel

Source: (Hassan, 2016).

2.4.5 Biogenic sources

HAp ceramic source from biogenic sources is thought to have better biocompatibility with living organs, because of its physicochemical similarity to the human bone hydroxyapatite and it is the cheap sources compared to the synthesis processes. There are few different types, including extraction of minerals from biowastes, synthesis from eggshells (Kamalanathan et al., 2014), synthesis from exoskeleton of marine organisms (Alif, Aprillia, & Arief, 2018; Rujitanapanich, Kumpapan, & Wanjanoi, 2014), synthesis with the aid of natural biomolecules, and synthesis using bio membranes (Sadat-shojai et al., 2013). Preparation of HAp using biowastes like bovine bones and fish bones usually involves a few hours annealing during which the organic materials in the bone get removed, leaving pure HAp as the residue. However the thermal process will produce the macrosize particles of the Hap (Jayachandran Venkatesan, Qian, & Ryu, 2011). An alternate method of alkaline hydrolysis was use to synthesis the pure nHA fish bone (Venkatesan, 2015). Calcium carbonate (calcite) is the primary component in eggshells and it makes up about 94% of chemical composition of eggshell. This makes the egg shells an essential material for hydroxyapatite production (Abdulrahman et al., 2014)**.** HAp is also smaller in size and cellular response to HAp will depend on the particle size and smaller particles will have more advantages over larger particles. The cellular response also depends on morphology, crystallinity, and chemical composition (Akram, 2014). In medical application, amorphous Hap is less use as a bone graft because of its very fast dissolution rate. Recent studies show that, the high degree of crystallinity around 60-70% and the nano size particles will reduce the resorbability of HAp (Poralan, 2015).

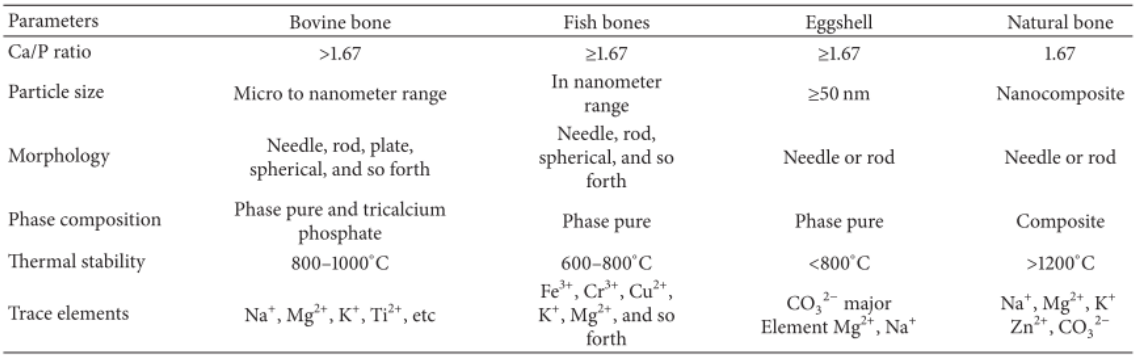

Parameters	Bovine bone	Fish bones	Eggshell	Natural bone
Ca/P ratio	>1.67	≥1.67	≥1.67	1.67
Particle size	Micro to nanometer range	In nanometer range	≥50 nm	Nanocomposite
Morphology	Needle, rod, plate, spherical, and so forth	Needle, rod, spherical, and so forth	Needle or rod	Needle or rod
Phase composition	Phase pure and tricalcium phosphate	Phase pure	Phase pure	Composite
Thermal stability	800–1000°C	600–800°C	<800°C	>1200°C
Trace elements	Na^+, Mg^{2+}, K^+, Ti^{2+}, etc	Fe^{3+}, Cr^{3+}, Cu^{2+}, K^+, Mg^{2+}, and so forth	CO_3^{2-} major Element Mg^{2+}, Na^+	Na^+, Mg^{2+}, K^+ Zn^{2+}, CO_3^{2-}

Figure 2-9: Different source of HAp synthesis

Source: (Poralan, 2015)

2.5 Fish

Figure 2-10: *Scomber scombrus*

Most of the world's large fish populations are pelagic. They include the highly migratory species of tuna, herring (*Clupea harengus*) and mackerel (*Scomber scombrus*), and smaller species such sardines and anchovy. With 75% of the global fish production meant for direct human consumption, it has maintained its importance as the top protein provider in the diet of many nations in the world. This essentially means that in 1970 an average Malaysian consumed more fish (20kg/year) compared to 54kg in 2010, a dramatic increase in demand for fish over four decades that is compounded by rapid population growth. Pelagic fishes are the important contributor for fishier. Pelagic fish normally spend most of the life swimming in the water column (seas, oceans or open waters which associated with the surface or middle depths of a water body) with little contact with or dependency on the bottom of the sea floor. Many pelagic fish food source is plankton. The most common pelagic fishes found in Malaysian seas include mackerel, tuna and sardines

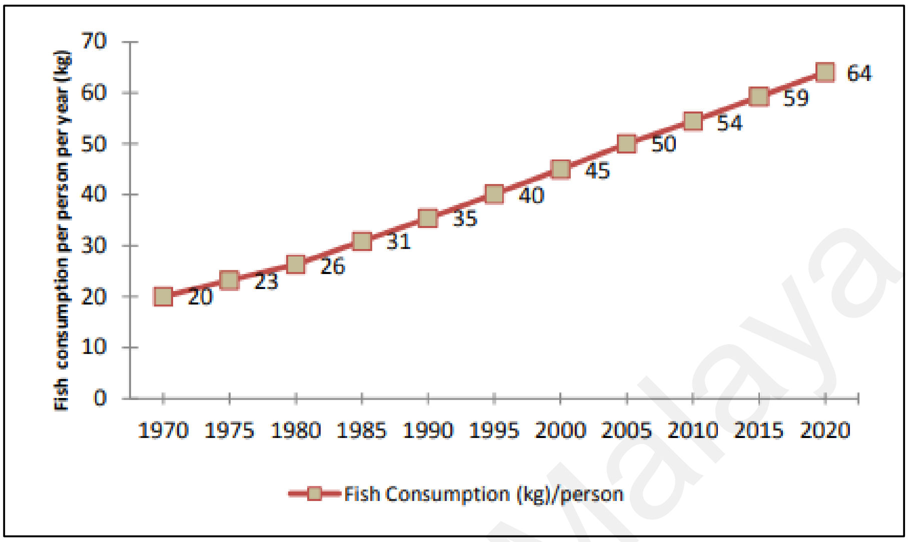

Figure 2-11: Fish consumption of an average Malaysia from 1970 to 2020

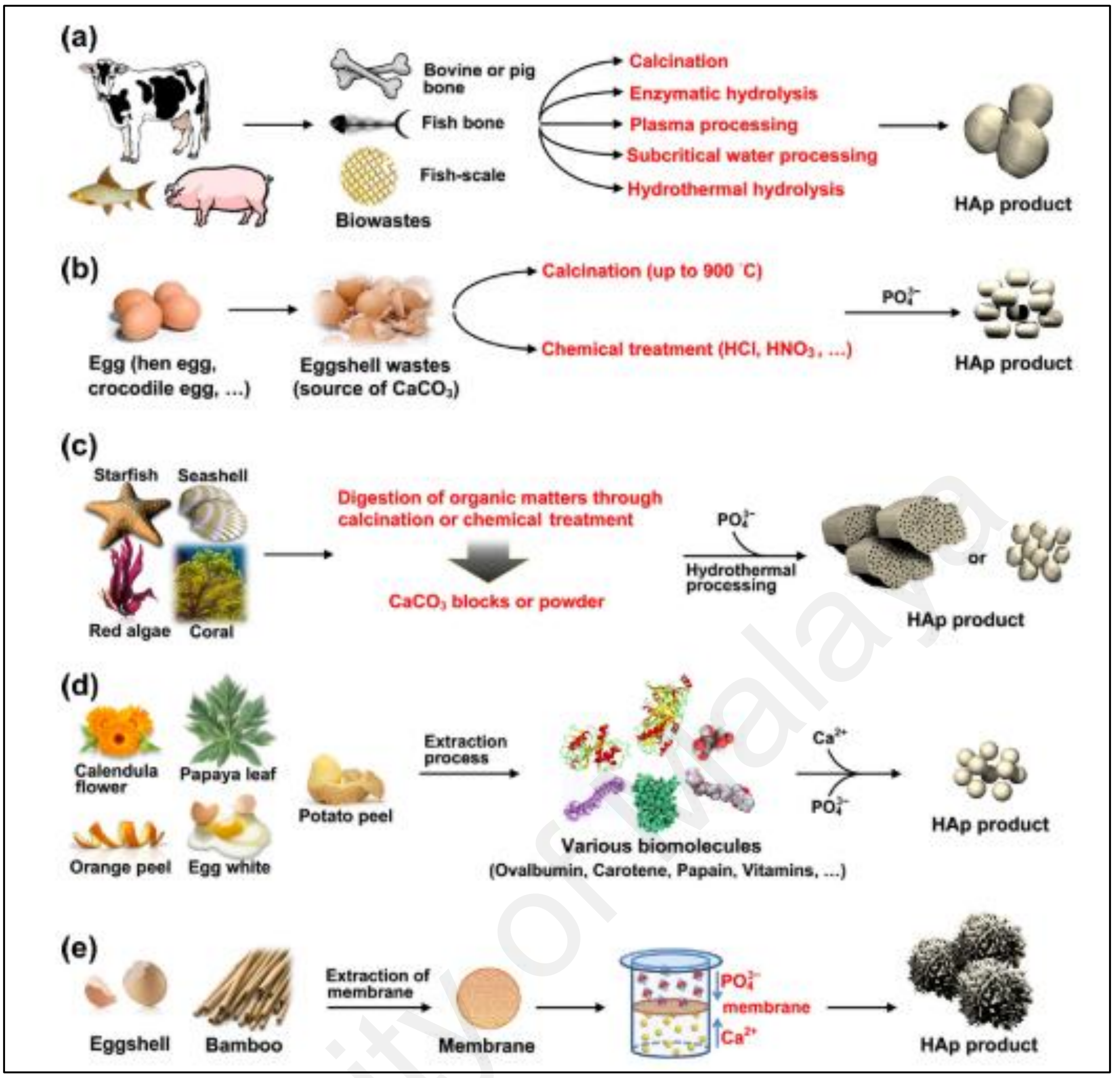

Figure 2-12: Source of the HAp from waste material

Source:(Sadat-shojai et al., 2013)

CHAPTER 3: METHODS AND MATERIAL

3. Methods and materials

3.1 Introduction

This chapter describes the process and equipment by which fish bone was harvested from waste fish bone and processed into hydroxyapatite powder using sintering method. This process included cutting the raw fish bone, boiling to remove protein from the bones and finally sintering at different temperature. In addition to this, characterization and mechanical properties of the as-sintered samples were undertaken by x-ray diffraction (XRD), Scanning electron miscopy (SEM), Fourier transform infrared spectroscopy (FTIR) analysis, Thermogravimetric analysis (TGA) analysis, Vickers hardness and fracture toughness determination. The process flow of the work is schematically shown below.

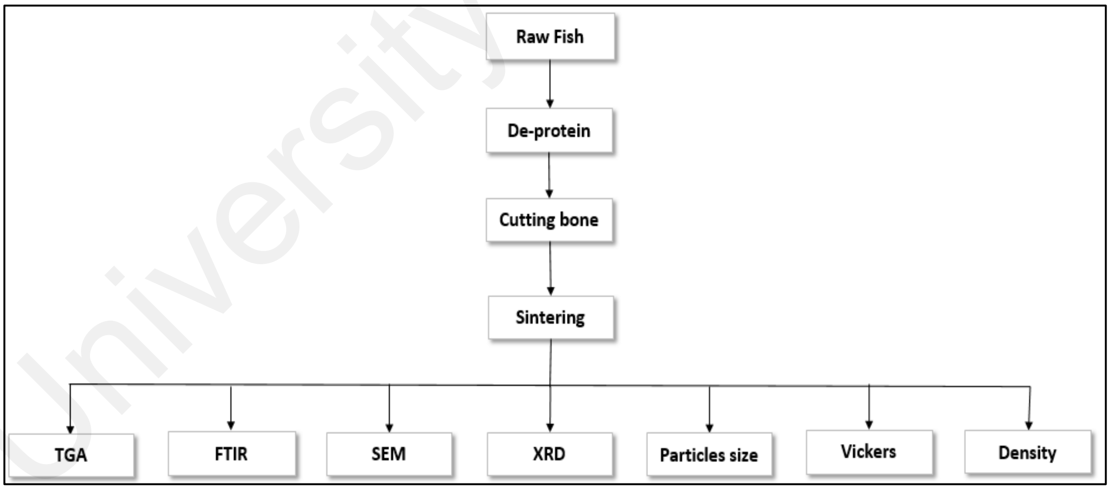

Figure 3-1: Process flow chart of characterization

3.2 Hydroxyapatite powder preparation:

The hydroxyapatite was extracted from fish bone. The purchased fish bone was cleaned from flesh and blood tissues on the bone. The cleaned fish bone was boiled in distilled water for 3h to remove all the protein flesh and blood. After the bone cleaned, the bone again boiled in distilled water for another 2h. The boiled bone samples were dehydrated in an oven at 60 ˚C for 6 h and stored the raw bones in the dry condition. After that, dried specimens were calcined for 5h in an electric furnace at different temperature 400 ˚C, 600 ˚C, 800 ˚C, 1000 ˚C, 1200 ˚C using a temperature rate of 5 ˚C /min under ambient condition to remove the organic substances and samples were label number 1,2,3,4,5 respectively. The samples were cooled until they reached room temperature by slow furnace cooling. Then the calcined bones were crushed into powder by mortar pestle. The powder was used for XRD analysis, SEM, FTIR, Density analysis and particles size analysis. Figure 3-2 above shows the sequence of the HAp synthesis.

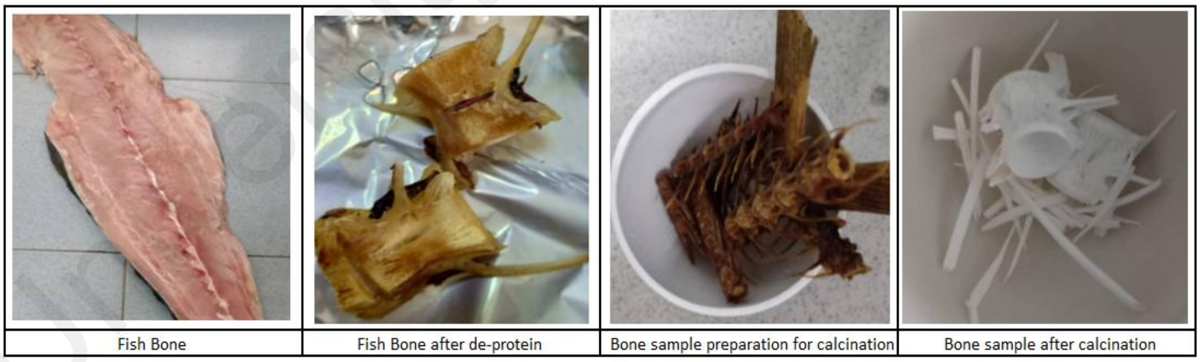

Figure 3-2: Sequence of the HAp synthesis process

3.3 Pelletised Hap powder preparation:

Dried fish bones were calcined in an electric furnace at temperature 800 ˚C using a temperature rate of 5 ˚C /min under ambient condition. The temperature was kept constant for 5h. The sample was cooled in the furnace until they reach the room temperature. Then the calcined bone were crashed by using mortar pestle into powder form. Around 2g of Fish bone-HAp powder was uniaxially pressed for 5 minute at 6 tons using a cylindrical die with a 20 mm diameter. The compacted green body was pressurelessly sintered in air atmosphere at temperature of 800 ˚C, 900°C, 1000 ˚C, 1100°C and 1200 ˚C, 1300°C with a furnace ramp rate of 5 ˚C/min and dwell time of 5 h. In order to obtain a smooth surface for indentation in vickers the surface of the sample was polished with a sand paper and clothes having a mesh size of 1 μm.

3.4 Thermal analysis:

Thermogravimetric analysis (TGA) is the test that carried out using an instrument knon as a thermogravimetric analyser. A thermogravimetric analyser continuously measures mass changing while the temperature of a sample is increase over time. Mass, temperature, and time in thermogravimetric analysis are considered base measurements. A TGA was used for bone characterization through analysis of characteristic decomposition patterns. The transformation process of fish bone into hydroxyapatite powder were studied by using a TG/DTA analyser (Setaram Setsys Evolution, France; operating range of 25 to 1090 °C). The thermogravimetric analysis (TGA) and differential thermal analysis (DTG) of the fish bone samples were recorded from 90 ˚C to 1200 ˚C at a heating rate of 5 ˚C/min in an air condition and the process shown in figure 3-4 below. The sample of 17mg of raw fish bone was crushed into small size before placing it inside in the TGA analyser. A detailed schematic of the TGA is shown in figure 3-3 below.

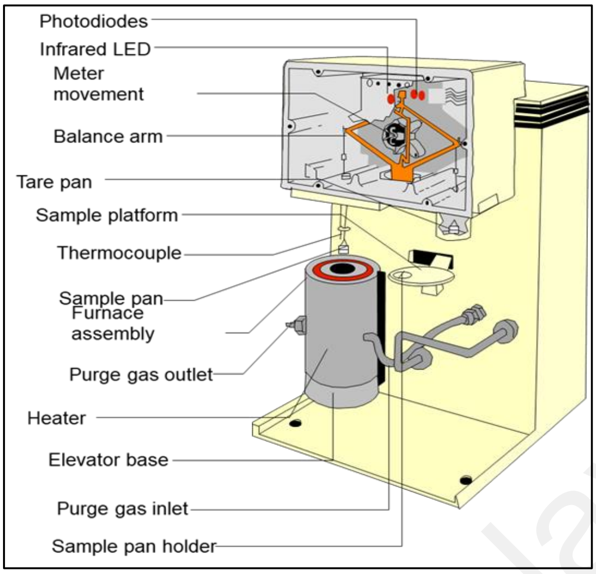

Figure 3-3: A detailed schematic of the TGA

Figure 3-4: Procedure of TGA

3.5 Density measurement

Bulk density measurement of sintered samples was calculated using distilled water as an immersion medium based on the Archimedes principal. The important part of characterizing the physical properties of ceramics is the accuracy of density measurements. Archimedes' technique which is liquid displacement method was used to determine the density of fired pellets. Measurements of the dry, saturated, and suspended weight are used to calculate the bulk density. Bulk density is the mass of an object divided by the bulk volume, V_b, the volume of solid plus all open and closed pores. According to the Archimedes' theorem, the bulk density can be calculate based on the following formulation:

The bulk density (ρ) of sintered sample is calculated using following equation:

$$\rho = \frac{W_{dry}\rho_w}{W_{sat} - W_{susp}}$$

Where:

W_{dry}= Dry weight of sample

W_{susp}= Suspended weight of sample

W_{sat}= Saturated weight of sample

ρ_w= Density of distilled water

The relative density density of each sample was calculated by taking the theoretical density of hydroxyapatite as 3.156g/cm3 (Karimzadeh, Ayatollahi, Bushroa, & Herliansyah, 2014).

3.5.1 Dry weight of sample

The sintered sample at different temperature was immediately weighted at weight scale to obtain the dry weight of the pallets with open pores. Usually, the dry weight is determined before saturation process.

3.5.2 Saturated weight of sample

Pellets were weighed at dry condition, then saturated with distilled water under vacuum until all bubbling removed. The sample were soaked in the water in vacuum condition for 2hr to make sure all the open pores fill up with the water. The saturated sample then remove from the water and remove the excess water on the pallets using the wet cloth. The sample were weighted and recorded.

3.5.3 Suspended weight of sample

The saturated pallets were suspended in the distilled water and the weight of sample were recorded. All the pores condition is shown as figure 3-5.

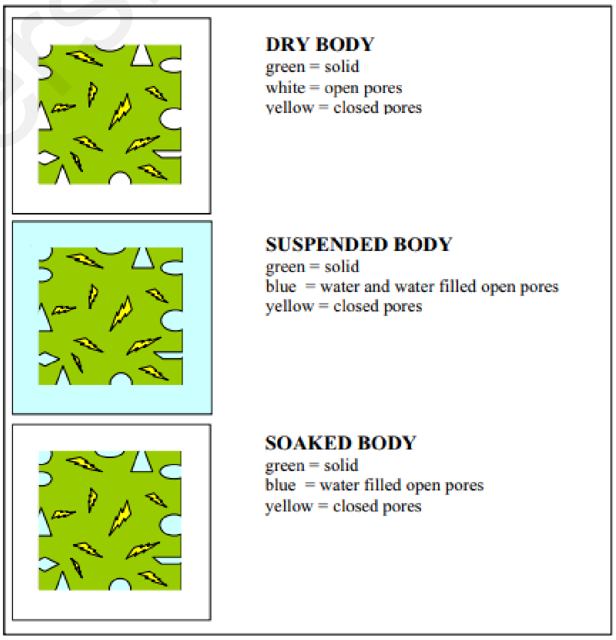

Figure 3-5: Dry, soaked and suspended bodies

3.6 FTIR

FTIR stands for Fourier transform infrared, the preferred method of infrared spectroscopy. Some radiation is absorbed by the sample and some passes through (is transmitted) when IR radiation is passed through a sample. The resulting signal at the detector is a spectrum representing a molecular ‘fingerprint’ of the sample. The usefulness of infrared spectroscopy arises because different chemical structures (molecules) produce different spectral fingerprints. The sample of FTIR can be solid, powder and liquid. However the powder need special sample preparation before it can used in the FTIR. Here is the preparation method:

1) Transfer some KBr into a mortar and crush it into powder.
2) Add about 1-2 % of HAp powder and mix well with KBr powder.
3) The mixture is now place in a stainless die that assembled as per the following figure.
4) Apply 8 to 10 ton of pressure for 3 to 5 minutes. Leave the vacuum on during this process.
5) Slowly depressure from the die and open the bleed screw and remove the disk from the die.
6) Using tweezers transfer the pressed HAp mixture pellet to the appropriate disk holder for IR analysis. Avoid contact with fingers as the pallet may contaminated.

./

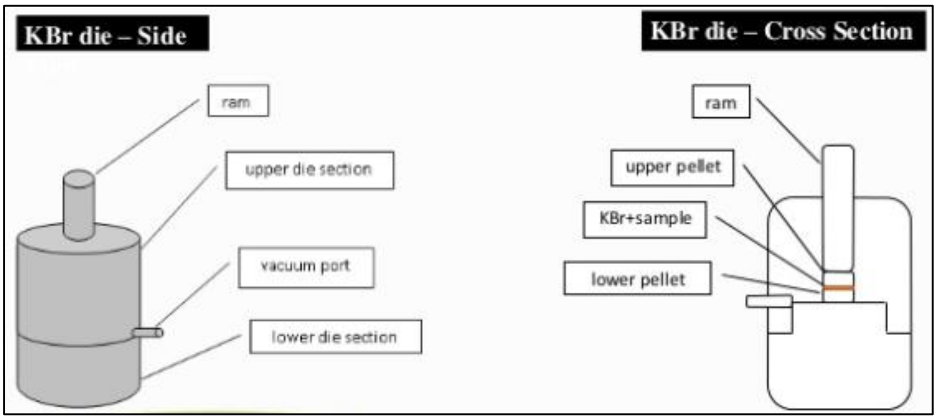

Figure 3-6: FTIR sample preparation

3.7 Vickers hardeness

The Vickers hardness of the sintered HAp was obtained using a pyramidal diamond indenter. The Vickers micro hardness test used a diamond tip, in the form of a square – based pyramid by applying 50g onto the polished surface of the sintered pellet sample. During the test, the load was applied smoothly, without impact and was maintained for 10 second. Five indentations were made for each sample and an average value was taken. The indentation for fracture toughness was measured using equation derived by Niihara (Rocha-Rangel, 2011).

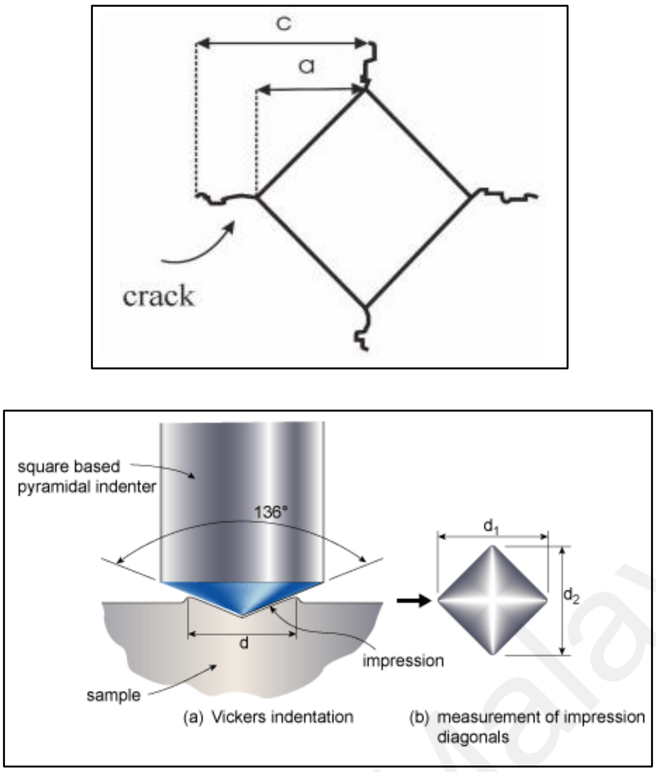

(a) Vickers indentation (b) measurement of impression diagonals

Figure 3-7: Hardness parameters

$$\mathrm{K_{ic}} = 0.16\left(\frac{\mathrm{c}}{\mathrm{a}}\right)^{-1.5}(Ha^{0.5}) \qquad\qquad H = 1.8\frac{P}{a^2}$$

Where:

$\mathrm{K_{IC}}$ = Fracture toughness ($\mathrm{MPa \cdot m^{1/2}}$)

H = Vickers hardness (MPa)

P = Test load in Vickers hardener (MPa)

c = Average length of the cracks obtained in the tips of the Vickers marks (microns)

a = Half average length of the diagonal of the Vickers marks (microns)

3.8 XRD

The X-ray diffraction (XRD) pattern of the final HAp nanoparticles was obtained with CuKa radiation (λ=0.15406 nm) on a diffractometer (RIGAKU MINIFLEX at AMU). The XRD patterns were recorded in a 2Ɵ range of 20˚ to 60˚ with a step size of 0.02˚ and scan speed of 0.5˚/min. The standard JCPDS cards used as a reference to identified the crystalline phases. The calcium (Ca) to phosphorus (P) ratio of sintered samples was calculated from compounds containing both elements. The mean crystallite size (D) of the particles was calculated from XRD line broadening measurement using the Scherrer equation (Abidi & Murtaza, 2014).

$$D = \frac{0.89\,\lambda}{\beta\cos\Theta}$$

Where

λ= The wavelength of CuKa,

$\boldsymbol{\beta}$= The full width at half maximum of the HA line and

Ɵ= The diffraction angle

3.9 SEM

Microstructural evolution under the various sintering temperatures was analysis using scanning electron microscopy (SEM, Phenom ProX desktop). The samples were mounted on aluminium stubs and subsequently coated with Au/ Pd (Polarons SC 7610, Fision Instruments). Chemical composition analysis was also carried out using energy dispersive X-ray spectroscopy (EDX) at 30.0 kV. Figure shows the sample preparation for SEM analysis.

Figure 3-8: SEM sample preparation

CHAPTER 4: RESULT AND DISCUSSION

4. Result and discussion

This chapter will present the results and discussions on the characterization technique and mechanical properties of the sintered fish bone as a source for producing the natural hydroxyapatite.

4.1. Calcination:

Table 4-1: Calcination reduction weight

Sample	Calcination Temperature (°C)	Calcination Period (°C)	Initial weight (g)	After calcination weight (g)	Residue (%)	Sample apparence
1	400	5	7.0272	5.0771	28%	Black
2	600	5	7.0974	4.834	32%	Grey
3	800	5	7.0759	3.1741	55%	White
4	1000	5	7.019	3.1027	56%	White
5	1200	5	7.0893	3.109	56%	White

Sample	1	2	3
Picture			

Sample	4	5
Picture		

Figure 4-1: The calcination initial and final mass

The above figure 4-1 shows the calcination appearance result at different temperature. It turned to black when at a calcination temperature of 400°C, which indicate 5 residue of organic compounds or presence of carbon due to incomplete combustion. In general, as the temperature increases, the bones turn grey at 600°C, white at 800°C,1000°C and 1200°C that shows the minerals compound in the bones. The decline in the yield on the calcination process is due to the loss of water and organic material contained in the powdered fish bones. The residual percentage is around 55-56 % at temperatures 1000°C and 1200°C. The calcination method was used to synthesis the Hydroxyapatite from fish bone (*Scomber scombrus*). In this research the cheap and easy method of calcination was successfully used to synthesis the HAp. Calcination was carried out at different temperature to investigate the changes in the microstructural and also mechanical properties. Form the calcination result, it shows that the fish bone turned to white at temperature of 800°C,1000°C and 1200°C. This shows that, above 800°C the organic compounds inside the fish was decomposed and leave the mineral Hydroxyapatite.

4.2. Thermogravimetric analysis (TGA)

About 16mg of the samples was used for the TGA experiment. Calcination result also supported by the TGA analysis where after temperature 690 ˚C, there is small weight loss and no significant changes in the DTG.

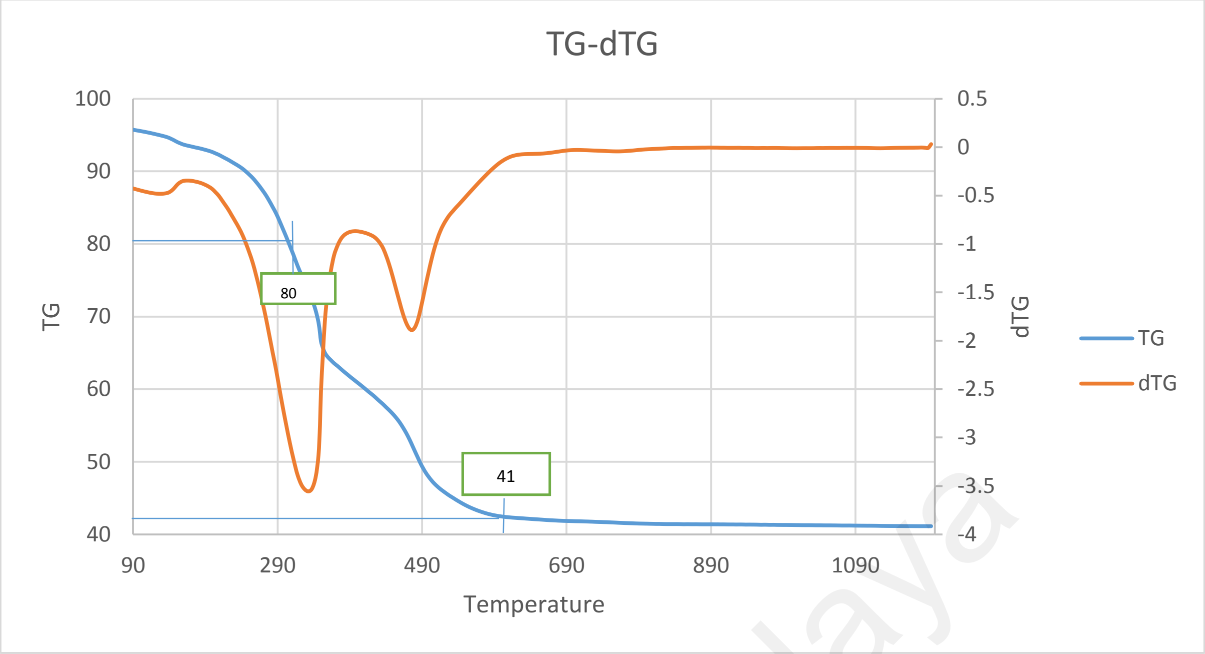

Figure 4-2: TGA analysis graph of untreated fish bone

The TGA analyses (90 ˚C –1090 ˚C) of raw fish bone using air at 5 ˚C/min is showed in Figure 4-2. Two different areas of weight loss (350˚C and 492˚C) were showed in the TGA spectrum of raw fish bone. Those temperatures correspond to the organic removal. It was shows in literature that between 400˚C - 600˚C heating temperature will lead to decomposition of CO_3^{2-} in air. This agreed with the result showed in this study and it indicates that the synthesized material HAp exhibits certain percent of CO_3^{2-} ions (Ulfyana et al., 2017). It is worthy of note that on the overall, there was no much pronounced weight loss due to endothermic and exothermic reaction in spectrum of the treated sample. This is an indication of good thermal stability of the obtained material as expected of chemical HAp. The overall weight loss of sample after 600 ˚C is around 59%. From literature review, it was reported that bone generally consists of about 30-40% organic components and about 60-70% inorganic components (J Venkatesan, 2013). Therefore, the higher amount of weight loss recorded for the untreated sample can be attributed to the presence of larger percent of organic constituents in the untreated bone powder compared with the treated sample. The DTG have revealed two exothermic peaks around 300-400˚C and 400-500˚C for which all are related to the changes in mass of the material. First exothermic peak could be due to desorption of water at surface, and further hike up temperature to 400°C cause of the elimination of interstitial water in crystal lattice. The second exothermic behaviour may represent the decarboxylation of the HAP sample where all the protein content burned out and leave the mineral component only (Meejoo, Maneeprakorn, & Winotai, 2006).

4.3. FTIR analysis

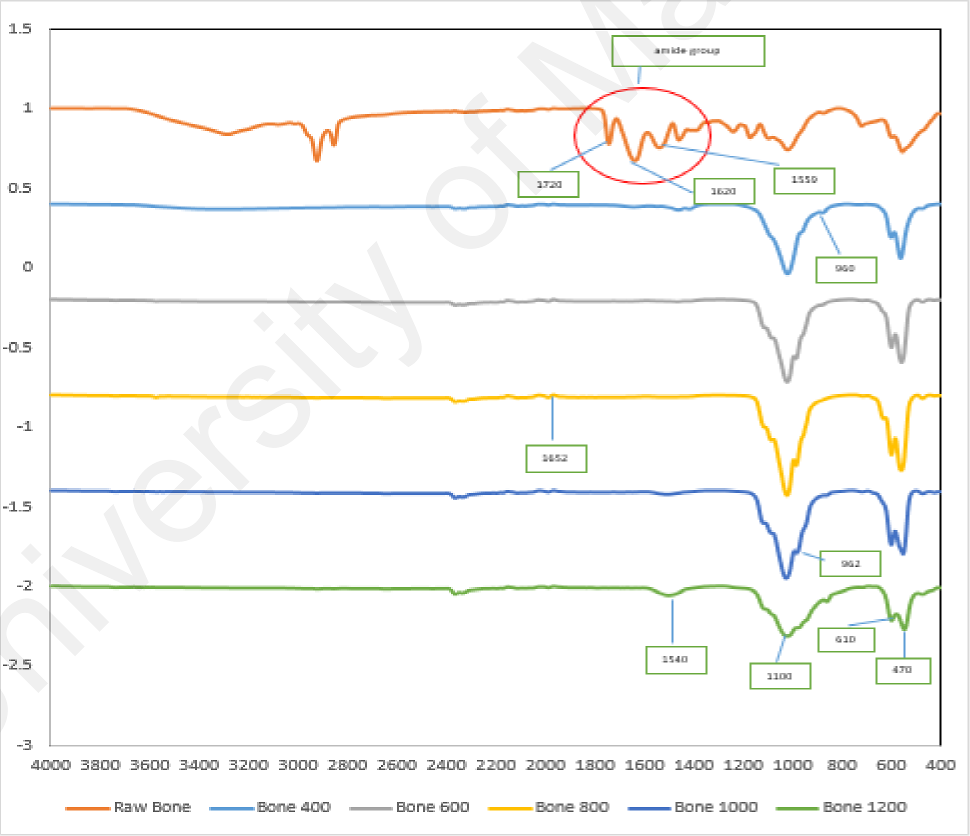

Figure 4-3: FTIR analysis graph calcinated samples at 400°C, 600°C, 800°C, 1000°C, and 1200°C

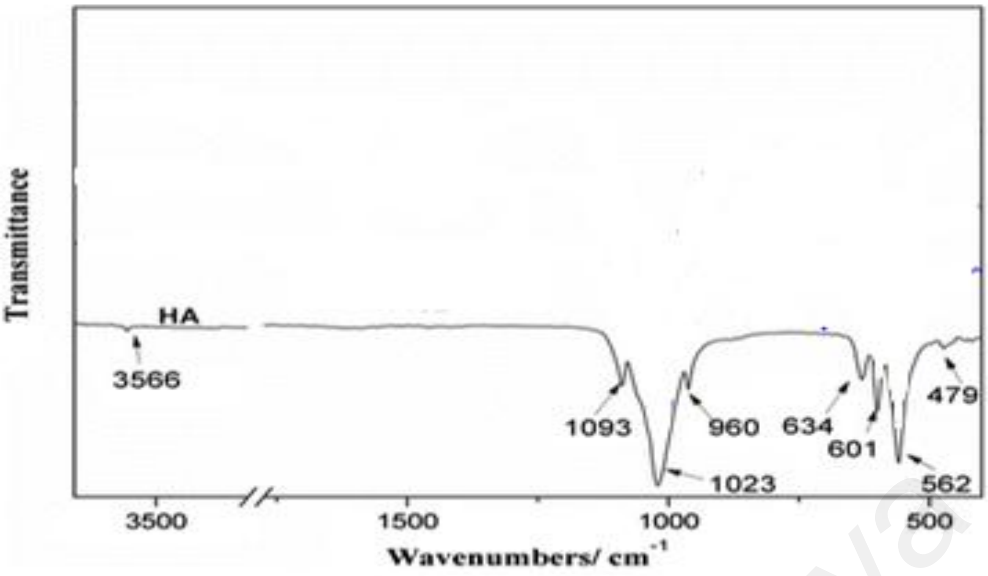

Figure 4-4: Standard FTIR graph of HAP

The FTIR analysis of all HAp powders is given in figure 4-3. The results showed that all the annealed fish bone exhibited FTIR spectrum that corresponded to stoichiometric HAp and agreed with the standard shape of the hydroxyapatite spectrum that shown in the figure 4-4. Moreover, it was observed that all the HAp powders spectrum has bands belonging to PO_4^{3-} group at 470 cm^{-1}, 560–610 cm^{-1}, 960 cm^{-1} and 1000–1100 cm^{-1} (Ramesh et al., 2013) . The FTIR bands of HAp have been investigated. The organic material contain protein that can be detected by FTIR analysis in three main amide bands: amide group. Amide I shows the bands at 1620, 1636 and 1685cm^{-1}. For the raw fish bone, the three bands clearly confirmed from the second derivative curve of the original spectra. However, these bands not seen in the spectra of the treated bones after thermal calcination. Amide II band has major peak at 1559cm^{-1} and there are minor bands at 1521, 1533 and 1543cm^{-1}. The amide peaks did not shown in the treated fish bones which confirmed that the calcinated bones around 600˚C are free from amide group like protein and collagen (Sheikh & Yong, 2008, Pal et al., 2017). Thus colour change from black at 400 ˚C to grey at 600 ˚C and finally white at 800 ˚C indicate the removal of organic material completely. Therefore, there are no much changes observed in the FTIR spectra of bones calcinated from 800 ˚C to 1200 ˚C, suggesting no composition changes due to thermal effect. In general, the FTIR spectra indicate the presence of phosphate (PO_4^{3-}), hydroxyl (OH^-) and carbonate (CO_3^{2-}) ions in calcinated fish bones. The 1000-1100 cm^{-1} bands arise from ν_3 PO_4^{3-}, the 962 cm^{-1} band arises from ν_1 PO_4^{3-}, and the 610 cm^{-1} bands arise from ν_4 PO_4^{3-} (Ramesh, 2007). The carbonate ions peaks is around 1650 cm^{-1} while bands around 960 cm^{-1} shows the presence of β-type tricalcium phosphate (TCP) (Danial Aminin bin Zairin, 2017).

Temperarture ˚C	**Chemical groups and phase**	**Absorption Bands, (cm-1)**	**Description**
400	Amides group	1620,1559 and 1720	The protein group and impurities
600	carboxyl group	1450	Disapper
800	***β***-TCP	962 and 1120	***β***-TCP shoulders begin to how up
1000	phosphate group	470, 560–610 and 1000–1100	Shift position at of phosphate group
1200	***β***-TCP		More ***β***-TCP done the HA

Figure 4-5: FTIR graph analysis

Source: (Meejoo et al., 2006)

4.4. EDX analysis

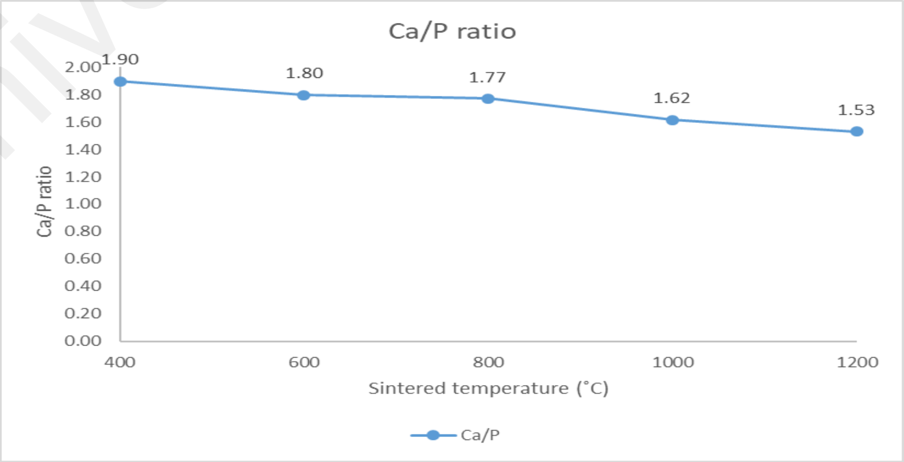

Figure 4-6: Ca/P ratio graph (EDX)

<table>
<tr><th>Temp</th><th>Image</th><th>EDX</th><th>Ca/P ratio</th></tr>
<tr><td>400</td><td>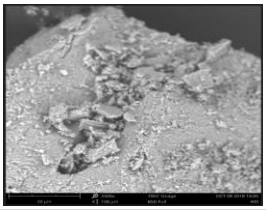</td><td>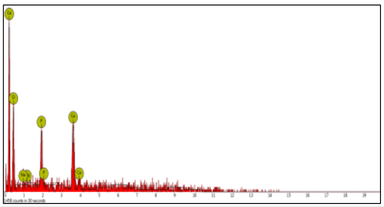</td><td><table>
<tr><th>Element Symbol</th><th>Atomic Conc.</th><th>Weight Conc.</th><th>Oxide Symbol</th><th>Stoich. wt Conc.</th></tr>
<tr><td>O</td><td>58.52</td><td>47.56</td><td></td><td></td></tr>
<tr><td>Ca</td><td>13.81</td><td>28.12</td><td>Ca</td><td>53.62</td></tr>
<tr><td>C</td><td>19.66</td><td>12</td><td>C</td><td>22.88</td></tr>
<tr><td>P</td><td>7.28</td><td>11.46</td><td>P</td><td>21.85</td></tr>
<tr><td>Na</td><td>0.38</td><td>0.44</td><td>Na</td><td>0.84</td></tr>
<tr><td>Mg</td><td>0.34</td><td>0.42</td><td>Mg</td><td>0.81</td></tr>
<tr><td>CA/P</td><td>1.90</td><td></td><td></td><td></td></tr>
</table></td></tr>
<tr><td>600</td><td>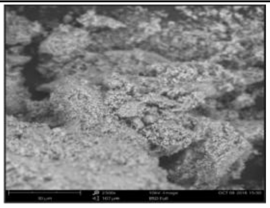</td><td>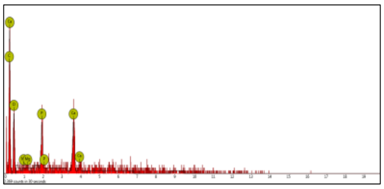</td><td><table>
<tr><th>Element Symbol</th><th>Atomic Conc.</th><th>Weight Conc.</th><th>Oxide Symbol</th><th>Stoich. wt Conc.</th></tr>
<tr><td>C</td><td>58.24</td><td>46.8</td><td>C</td><td>75</td></tr>
<tr><td>O</td><td>35.14</td><td>37.61</td><td></td><td></td></tr>
<tr><td>Ca</td><td>4.69</td><td>9.35</td><td>Ca</td><td>14.99</td></tr>
<tr><td>P</td><td>2.61</td><td>5.41</td><td>P</td><td>8.67</td></tr>
<tr><td>Mg</td><td>0.26</td><td>0.42</td><td>Mg</td><td>0.67</td></tr>
<tr><td>Na</td><td>0.27</td><td>0.41</td><td>Na</td><td>0.66</td></tr>
<tr><td>CA/P</td><td>1.80</td><td></td><td></td><td></td></tr>
</table></td></tr>
<tr><td>800</td><td>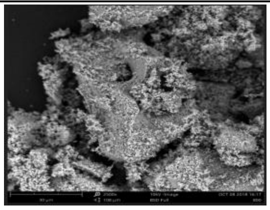</td><td>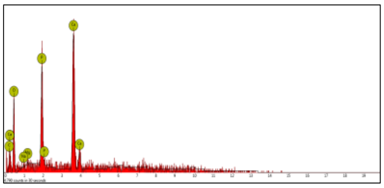</td><td><table>
<tr><th>Element Symbol</th><th>Atomic Conc.</th><th>Weight Conc.</th><th>Oxide Symbol</th><th>Stoich. wt Conc.</th></tr>
<tr><td>C</td><td>63.3</td><td>54.07</td><td>C</td><td>87.88</td></tr>
<tr><td>O</td><td>33.81</td><td>38.48</td><td></td><td></td></tr>
<tr><td>Ca</td><td>1.77</td><td>5.05</td><td>Ca</td><td>8.21</td></tr>
<tr><td>P</td><td>1</td><td>2.21</td><td>P</td><td>3.6</td></tr>
<tr><td>Mg</td><td>0.11</td><td>0.19</td><td>Mg</td><td>0.31</td></tr>
<tr><td>Na</td><td>0</td><td>0</td><td>Na</td><td>0</td></tr>
<tr><td>CA/P</td><td>1.77</td><td></td><td></td><td></td></tr>
</table></td></tr>
<tr><td>1000</td><td>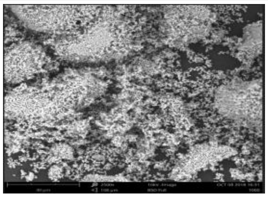</td><td>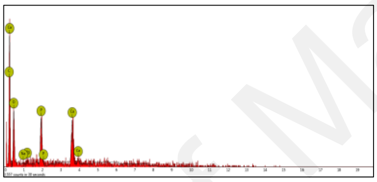</td><td><table>
<tr><th>Element Symbol</th><th>Atomic Conc.</th><th>Weight Conc.</th><th>Oxide Symbol</th><th>Stoich. wt Conc.</th></tr>
<tr><td>C</td><td>57.91</td><td>45.75</td><td>C</td><td>77.1</td></tr>
<tr><td>O</td><td>34.88</td><td>37.60</td><td></td><td></td></tr>
<tr><td>Ca</td><td>4.46</td><td>12.03</td><td>Ca</td><td>15.22</td></tr>
<tr><td>P</td><td>2.76</td><td>4.71</td><td>P</td><td>7.68</td></tr>
<tr><td>Na</td><td>0</td><td>0.00</td><td>Na</td><td>0</td></tr>
<tr><td>Mg</td><td>0</td><td>0</td><td>Mg</td><td>0</td></tr>
<tr><td>CA/P</td><td>1.62</td><td></td><td></td><td></td></tr>
</table></td></tr>
<tr><td>1200</td><td>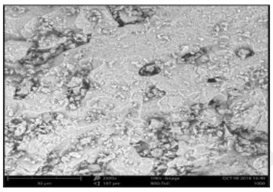</td><td>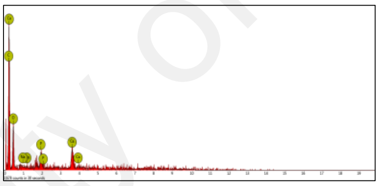</td><td><table>
<tr><th>Element Symbol</th><th>Atomic Conc.</th><th>Weight Conc.</th><th>Oxide Symbol</th><th>Stoich. wt Conc.</th></tr>
<tr><td>C</td><td>58.41</td><td>47.27</td><td>C</td><td>77.1</td></tr>
<tr><td>O</td><td>35.88</td><td>38.68</td><td></td><td></td></tr>
<tr><td>Ca</td><td>3.46</td><td>9.33</td><td>Ca</td><td>15.22</td></tr>
<tr><td>P</td><td>2.26</td><td>4.71</td><td>P</td><td>7.68</td></tr>
<tr><td>Na</td><td>0</td><td>0</td><td>Na</td><td>0</td></tr>
<tr><td>Mg</td><td>0</td><td>0</td><td>Mg</td><td>0</td></tr>
<tr><td>CA/P</td><td>1.53</td><td></td><td></td><td></td></tr>
</table></td></tr>
</table>

Figure 4-7: EDX component table

The morphology surface study of the fish bone after calcination at different temperature was carried out using the SEM. Images at 2500X magnification were compared between the samples. The 800 and 1000 ˚C sample show rod like shape of the morphology. While at calcination temperature of 1200˚C the particles fused together and there was some porosity. The SEM result shows that the particles are smaller and the grain size detail calculated was discussed in XRD result. Based on the EDX result shown at figure 4-7 the Ca/P ratio decreased from 1.90 at a temperature of 400˚C to 1.53 at temperature 1200 ˚C. For pure HAp the ratio should be 1.67 (Boutinguiza et al., 2012).

The pure HAp is formed between temperature of 800 ˚C and 1000 ˚C. At temperature 800 ˚C the Ca/P ratio is higher compared to the synthesis HAp due to presence of carbonate ions substituting phosphate group, indicating the presences of B-type HAp. Other authors who studies for other animal bones also resulted with higher Ca/P ratio than synthetic Hap. The carbonate ions substitution for phosphate is favoured for B-type HAp than A-type because it has been reported that is higher affinity of osteoblasts (bone cells) for cell adhesion (Seok, Hong, Young, & Kook, 2012). The presence of B-type HAp have been seen from FTIR analysis. Besides, the EDX analysis is coincident with XRD analysis claiming the presence of minor elements after calcination process. The IR characteristic bands of carbonate substitution in apatites should be: ν_3 at ~1465 cm^{-1} for type-B (CO_3 substituting for PO_4) and ν_3 band at ~1546 cm^{-1} for type A (CO_3 substituting for OH). The Ca/P ratio start to lower down to 1.62 and 1.53 at temperature of 1000 and 1200 respectively represents that samples are less stable than HAp (Ca/P=1.67) and decomposed to form of α-TCP (lower temperature) and β-TCP (high temperature) (Ramesh 2007) and all the Ca/P ratio is shown table 4-2 below. Based on the literature review the HAp (1.67) higher solubility than the TCP (Ebrahimi & Botelho, 2017).

Table 4-2: Calcium (ortho) phosphate compounds and their solubility product constants

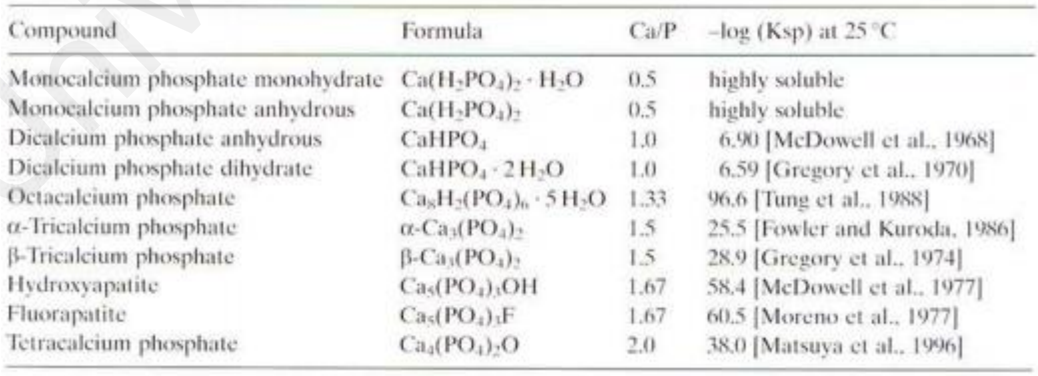

Compound	Formula	Ca/P	–log (Ksp) at 25 °C
Monocalcium phosphate monohydrate	$Ca(H_2PO_4)_2 \cdot H_2O$	0.5	highly soluble
Monocalcium phosphate anhydrous	$Ca(H_2PO_4)_2$	0.5	highly soluble
Dicalcium phosphate anhydrous	$CaHPO_4$	1.0	6.90 [McDowell et al., 1968]
Dicalcium phosphate dihydrate	$CaHPO_4 \cdot 2H_2O$	1.0	6.59 [Gregory et al., 1970]
Octacalcium phosphate	$Ca_8H_2(PO_4)_6 \cdot 5H_2O$	1.33	96.6 [Tung et al., 1988]
α-Tricalcium phosphate	$\alpha\text{-}Ca_3(PO_4)_2$	1.5	25.5 [Fowler and Kuroda, 1986]
β-Tricalcium phosphate	$\beta\text{-}Ca_3(PO_4)_2$	1.5	28.9 [Gregory et al., 1974]
Hydroxyapatite	$Ca_5(PO_4)_3OH$	1.67	58.4 [McDowell et al., 1977]
Fluorapatite	$Ca_5(PO_4)_3F$	1.67	60.5 [Moreno et al., 1977]
Tetracalcium phosphate	$Ca_4(PO_4)_2O$	2.0	38.0 [Matsuya et al., 1996]

Source: (Chow & Components, 2001)

4.5. Density

In the present study, the bulk density of the sintered HAp compact was obtained via the Archimedes' method where the distilled water was used as the immersion medium. The relative density of the sintered HAP compacts was then measured using the theoretical density of HAp as 3.14 g/cm3. The effect of sintering temperature on the relative density is shown in table 4-2. As shown in the figure 4-8 where a steady increase in relative density was observed as sintering temperature increase up to 1000°C and drop slight until 1200°C. The drop in the relative density above the 1000°C was attributed to the presence of detrimental secondary phases (α-TCP and β-TCP) in the sintered HAp (Kamalanathan et al., 2014). Based on the literature, the density, flexural strength and hardness of sintered bodies increased with sintering temperature and reached an optimum at around 1150 °C and then decreasing trend because of the decomposition of HAp into TTCP and TCP at higher temperature. On (Hung, Shih, Hon, & Wang, 2012) HAp change to β-TCP, which has a lower density around 3.06 g/cm^3 than HAp density is 3.14 g/cm^3. Increase the sintering temperature, cause the β-TCP transforms to α-TCP, which has a lower density of 2.81 g/cm^3 (Nath, Biswas, Wang, Bordia, & Basu, 2010). However, literature shows, that β-α-TCP transformation upon heating occurred at 1180°C, which was lower than that reported by Pierre as well as in this investigation. In the present case, β-α-TCP transformation in the composites occurred at and above 1200°C (Mackay, 1953). On the other hand, the densification of ceramics increase in a solid state as a sintering due to the process of pore elimination, with a shrinkage process through the transfer of matter from the particle volume or from the grain boundary between particles. Thus, it can be suggested that the transfer of matter from the particle volume was substantially enhanced with the sintering process in the present study (Hung et al., 2012).

Table 4-3: Relative Density Calculation

Relative density calculation							
Temperature (°C)	Dry Mass(g)	Saturated Mass(g)	Suspended Mass(g)	Distalled Water Density (g/cm3)	Density of HAP (g/cm3)	Relative density of HAP (%)	Apparent Porosity (%)
400	1.4991	2.0161	1.4631	0.9959	2.6997	86%	93%
600	1.522	1.9851	1.4731	0.9959	2.9605	94%	90%
800	1.494	1.8388	1.3518	0.9959	3.0552	97%	71%
1000	1.5459	1.9078	1.4098	0.9959	3.0915	98%	73%
1200	1.455	1.6085	1.1035	0.9959	2.8694	91%	30%

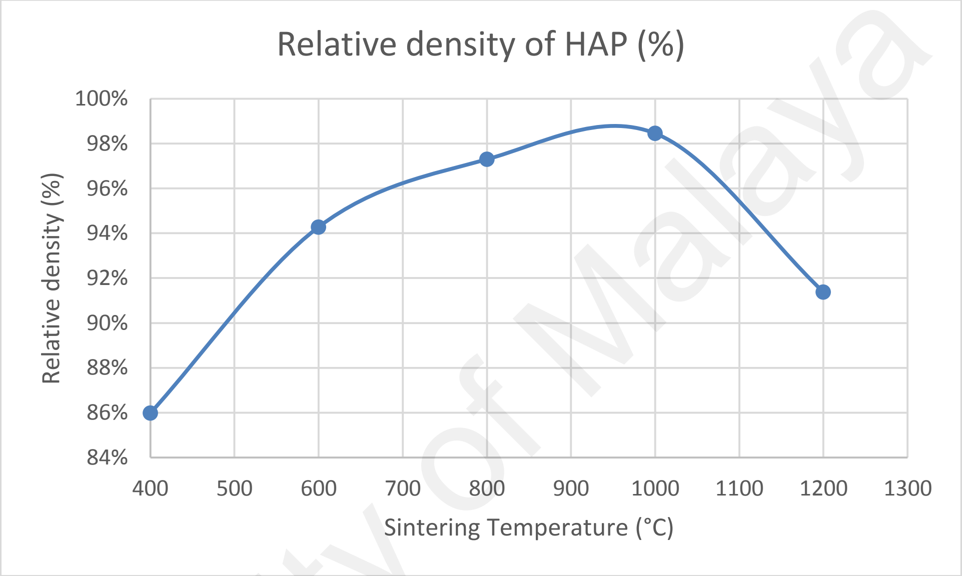

Figure 4-8: Relative Density graph

4.6. Hardness

Based on figure 4-9, the hardness of the sintered HAp rapidly increases from 0.49 GPa to 3.41 GPa when the sintering temperature increases from 800 °C to 1000 °C, then rapidly decreases to 1.16 when sintering at 1200 °C. The maximum hardness of the sintered HAp at 1000 °C. Hence, higher density let to higher hardness by the bonding amongst the grains in the sintered samples. The decrease of relative density and hardness may be associated with the decomposition of the HAp to TCP at higher temperature, thus resulting in poor densification and mechanical properties.

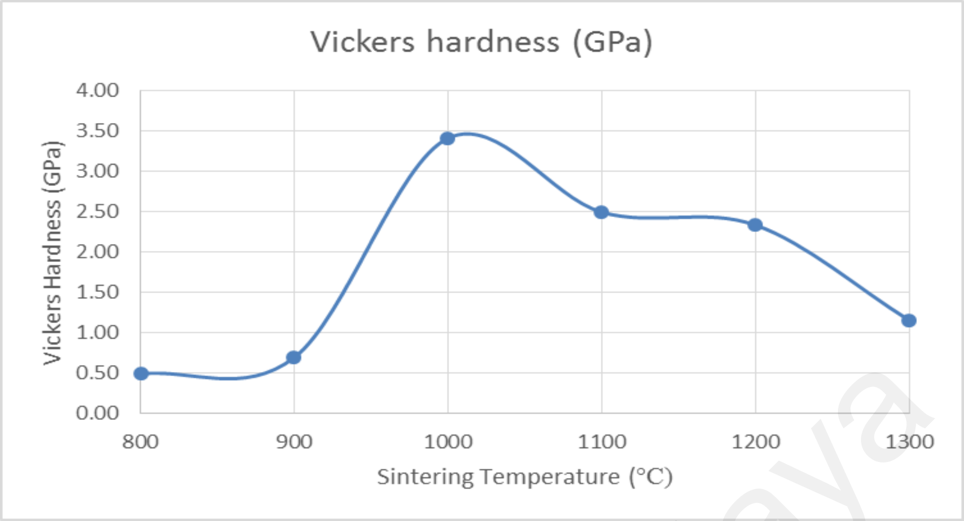

Figure 4-9: Vickers Hardness (GPa) graph

4.2. XRD

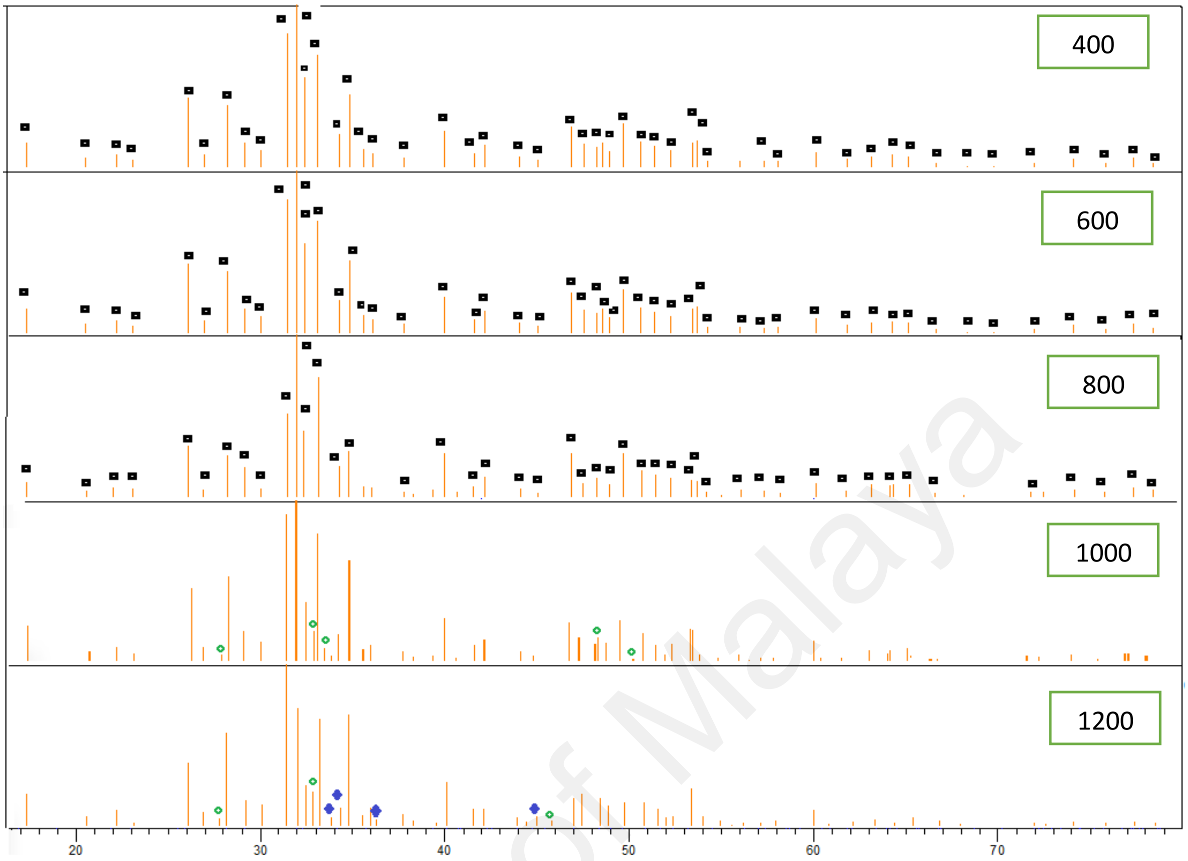

Figure 4-10: XRD analysis

■ :HAP
◇ :alpha- TCP
✦ :beta-TCP

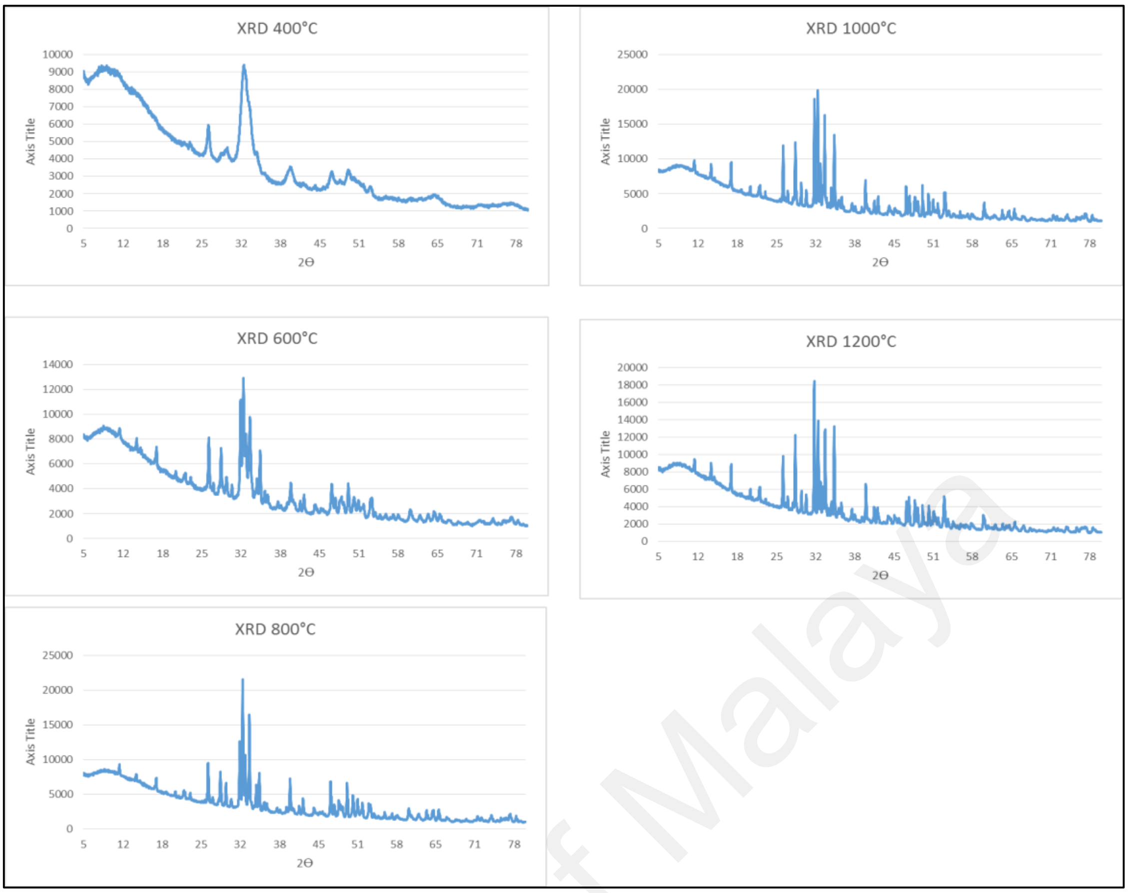

Figure 4-11: XRD analysis for temperature of 400°C, 600°C, 800°C, 1000°C, and 1200°C

Figure 4-11 depict the XRD patterns for the sintered samples of 400°C, 600°C, 800°C, 1000°C, and 1200°C respectively. The XRD exhibited a substantial increase in peak height and a decrease in peak width, thus indicating an increase in crystallinity and crystallite size (Ramesh, 2007). The obtained XRD spectra were compared to the JCPDS 09-0432 standard HAP data and shows the similarities in the fish bones. All the crystalline peaks in XRD spectra closely matched with peaks in standard HAp which means that the thermal process has produced natural HAp. The Bragg reflection at (002) planes of HAp is considered for calculation of the crystallite size (Mandal, 2016). The presence of tricalcium phosphate (TCP) phases in the sample sintered 1200 °C indicates the decomposition of HAp. As the annealing temperature increased to 1200 °C, the intensity of the characterized peaks for b-TCP, which is located at 2Ɵ angles was observed to gradually increase(Muralithran & Ramesh, 2000). It has been reported that when HAp sintered for 4h at temperature 1000°C and 1350 °C in air, it started to decompose and convert into β-TCP. The phase of TTCP appeared when sintering at temperature 1300 °C. Some of the β-TCP converted to α-TCP when sintering at higher temperature 1350 °C (Hung et al., 2012).

Table 4-4: The crystalline size of the HAp at different temperature

Temperature(°C)	**Peak position 2θ (°)**	**FWHM B_{size} (°)**	**Dp (nm)**
400	25.9969	0.2558	**31.87**
600	26.1027	0.5117	**15.94**
800	26.0826	0.4093	**19.92**
1000	26.09	0.1279	**63.76**
1200	26.0662	0.1279	**62.11**

CHAPTER 5: CONCLUSION

5. Conclusion

The present study aims at synthesizing and investigating the sinter ability of phase pure hydroxyapatite (HAp) via a thermal calcination route, using wasted fish bone as a source of HAp. In addition, the aptness of fishbone-derived HAp for clinical application in terms of its mechanical properties was assessed via Vickers hardness analysis. Apart from that, the physical characteristics of as-synthesized and sintered HAp were also evaluated in the current research.

Prior to synthesis of HA, he effects of calcination on the purity of HA extracted from waste wasted fish bone were investigated, as its usage in the synthesis of high purity HA is of paramount importance. The findings from the aforementioned investigation indicated that a calcination of fish bone beyond 800°c resulted in the formation of pure HAp, with the highest purity attained at 1000 °c. These result were confirmed via XRD and FTIR analysis on the calcinated sample.

Based on EDS analysis the synthesis of HAp exhibited a Ca/P molar ratio of 1.77 at 800°C which exceeding the molar ratio of the pure HAp of 1.667. The higher Ca/P molar ratio was attributed to the presence study was ascertained by XRD and ftir data, indicating the successful formation of HAp matrix in the synthesized powder.

In the present study, green compacted were formed and sintered within a temperature range of 800°C-1200°C to facilitate physical and mechanical property evaluation. Based on the findings from XRD and FTIR analysis, sintered compacts exhibited high thermal stability up to 1000°C. Sintering above 1000°C resulted in the decomposition of HAp. These results are parallel with the observation from SEM micrographs, where increased sintering temperature resulted in the presents of pore, thus forming a dense ceramic. Similar to synthesized HAp, sintered HAp compacted displayed Ca/P molar ratios greater than stoichiometric HAp within the range of 1.90-1.53.

In term of mechanical property evaluation, the hardness of sintered HAp increased from 0.49 GPa at 800°C to a maximum of 3.49GPa at 1000°C. Beyond this point, decomposition of HAp contributed to the decline in hardness.

REFERENCE

Abdulrahman, I., Tijani, H. I., Mohammed, B. A., Saidu, H., Yusuf, H., Jibrin, M. N., & Mohammed, S. (2014). From Garbage to Biomaterials : An Overview on Egg Shell Based Hydroxyapatite. *Journal of Materials*, *2014*(May), 6. https://doi.org/http://dx.doi.org/10.1155/2014/802467

Abidi, S. S. A., & Murtaza, Q. (2014). Synthesis and characterization of nano-hydroxyapatite powder using wet chemical precipitation reaction. *Journal of Materials Science and Technology*, *30*(4), 307–310. https://doi.org/10.1016/j.jmst.2013.10.011

Adzila, S., Sopyan, I., & Hamdi, M. (2011). Mechanochemical Synthesis of Hydroxyapatite Nanopowder: Effects of Rotation Speed and Milling Time on Powder Properties. *Applied Mechanics and Materials*, *110–116*, 3639–3644. https://doi.org/10.4028/www.scientific.net/AMM.110-116.3639

Akram. (2014). Extracting hydroxyapatite and its precursors from natural resources. *Journal of Materials Science*, *49*(4), 1461–1475. https://doi.org/10.1007/s10853-013-7864-x

Alif, M. F., Aprillia, W., & Arief, S. (2018). A hydrothermal synthesis of natural hydroxyapatite obtained from Corbicula moltkiana freshwater clams shell biowaste. *Materials Letters*, *230*, 40–43. https://doi.org/10.1016/j.matlet.2018.07.034

Anitha, P., & Pandya, H. M. (2014). Comprehensive Review of Preparation Methodologies of Nano Hydroxyapatite. *Journal of Environmental Nanotechnology*, *3*(1), 101–121. https://doi.org/10.13074/jent.2013.12.132058

Bakan. (2013). A novel low temperature sol-gel synthesis process for thermally stable nano crystalline hydroxyapatite. *Powder Technology*, *233*, 295–302. https://doi.org/10.1016/j.powtec.2012.08.030

Ben-Arfa. (2017). Novel route for rapid sol-gel synthesis of hydroxyapatite, avoiding ageing and using fast drying with a 50-fold to 200-fold reduction in process time. *Materials Science and Engineering C*, *70*, 796–804. https://doi.org/10.1016/j.msec.2016.09.054

Bose, S., & Tarafder, S. (2012). Calcium phosphate ceramic systems in growth factor and drug delivery for bone tissue engineering: A review. *Acta Biomaterialia*, *8*(4), 1401–1421. https://doi.org/10.1016/j.actbio.2011.11.017

Boutinguiza, M., Pou, J., Comesaña, R., Lusquiños, F., Carlos, A. De, & León, B. (2012). Biological hydroxyapatite obtained from fi sh bones. *Materials Science & Engineering C*, *32*(3), 478–486. https://doi.org/10.1016/j.msec.2011.11.021

Brzezi, J., Haberko, K., Sitarz, M., Bu, M., & Macherzy, B. (2015). Hydroxyapatite from animal bones – Extraction and properties, *41*, 4841–4846. https://doi.org/10.1016/j.ceramint.2014.12.041

Chow, L. C., & Components, G. (2001). Solubility of Calcium Phosphates, *l*.

Cox, S. (2014). Synthesis method of hydroxyapatite. *Lucideon, Insight Creating Advantage*, *1*(January 2014), 1–7.

Danial Aminin bin Zairin. (2017). Temperature Effect on Natural Hydroxyapatite Obtained from Fish Bones for Bone Tissue Engineering, 52.

Ebrahimi, M., & Botelho, M. (2017). Biphasic calcium phosphates (BCP) of hydroxyapatite (HA) and tricalcium phosphate (TCP) as bone substitutes: Importance of physicochemical characterizations in biomaterials studies. *Data in Brief*, *10*, 93–97. https://doi.org/10.1016/j.dib.2016.11.080

Hassan, M. A. (2016). A review of hydroxyapatite-based coating techniques: Sol-gel and electrochemical depositions on biocompatible metals. *Journal of the Mechanical Behavior of Biomedical Materials*, *57*, 95–108. https://doi.org/10.1016/j.jmbbm.2015.11.031

Hung, I., Shih, W., Hon, M., & Wang, M. (2012). The Properties of Sintered Calcium Phosphate with, *3*, 13569–13586. https://doi.org/10.3390/ijms131013569

Kamalanathan, P., Ramesh, S., Bang, L. T., Niakan, A., Tan, C. Y., & Purbolaksono, J. (2014). Synthesis and sintering of hydroxyapatite derived from eggshells as a calcium precursor. *Ceramics International*, *40*(10), 16349–16359. https://doi.org/10.1016/j.ceramint.2014.07.074

Karimzadeh, A., Ayatollahi, M. R., Bushroa, A. R., & Herliansyah, M. K. (2014). Effect of sintering temperature on mechanical and tribological properties of hydroxyapatite measured by nanoindentation and nanoscratch experiments. *Ceramics International*, 1–6. https://doi.org/10.1016/j.ceramint.2014.01.131

Mackay, a. L. (1953). A preliminary examination of the structure of α-Ca3(PO4)2. *Acta Crystallographica*, *6*(8), 743–744. https://doi.org/10.1107/S0365110X53002088

Mandal, N. (2016). Materials Characterization Fish scale derived hydroxyapatite scaffold for bone tissue engineering. *Materials Characterization*, *121*, 112–124. https://doi.org/10.1016/j.matchar.2016.09.034

Manoj, M., Subbiah, R., Mangalaraj, D., Ponpandian, N., Viswanathan, C., & Park, K. (2015). Influence of Growth Parameters on the Formation of Hydroxyapatite (HAp) Nanostructures and Their Cell Viability Studies. *Nanobiomedicine*, *2*, 2. https://doi.org/10.5772/60116

Markovic, S., Lukic, M. J., & Bracko, I. (2014). Synthetical bone-like and biological hydroxyapatites : A comparative study of crystal structure and morphology My IOPscience Synthetical bone-like and biological hydroxyapatites : a comparative study of crystal structure and morphology View the table of c, (June). https://doi.org/10.1088/1748-6041/6/4/045005

Meejoo, S., Maneeprakorn, W., & Winotai, P. (2006). Phase and thermal stability of nanocrystalline hydroxyapatite prepared via microwave heating. *Thermochimica Acta*, *447*(1), 115–120. https://doi.org/10.1016/j.tca.2006.04.013

Mehta, D., & George, S. (2014). Hydroxyapatite : Synthesis and Characterization, (June).

Muralithran, G., & Ramesh, S. (2000). The e € ects of sintering temperature on the properties of hydroxyapatite, *26*, 221–230.

Nath, S., Biswas, K., Wang, K., Bordia, R. K., & Basu, B. (2010). Sintering, phase stability, and properties of calcium phosphate-mullite composites. *Journal of the American Ceramic Society*, *93*(6), 1639–1649. https://doi.org/10.1111/j.1551-2916.2010.03662.x

Nayak, A. K. (2010). Hydroxyapatite Synthesis Methodologies : An Overview, *2*(2), 903–907.

Osterhoff. (2016). Bone mechanical properties and changes with osteoporosis. *Injury*, *47*, S11–S20. https://doi.org/10.1016/S0020-1383(16)47003-8

Pal, A., Paul, S., Roy, A., Krishna, V., Das, M., & Sinha, A. (2017). Synthesis of hydroxyapatite from Lates calcarifer fish bone for biomedical applications. *Materials Letters*, *203*, 89–92. https://doi.org/10.1016/j.matlet.2017.05.103

Poralan. (2015). X-ray diffraction and infrared spectroscopy analyses on the crystallinity of engineered biological hydroxyapatite for medical application. *IOP Conference Series: Materials Science and Engineering*, *79*(1). https://doi.org/10.1088/1757-899X/79/1/012028

Prakasam, M. (2015). Fabrication , Properties and Applications of Dense Hydroxyapatite : A Review, 1099–1140. https://doi.org/10.3390/jfb6041099

Pramanik. (2007). Development of high strength hydroxyapatite by solid-state-sintering process. *Ceramics International*, *33*(3), 419–426. https://doi.org/10.1016/j.ceramint.2005.10.025

Qi, Y., Shen, J., Jiang, Q., Jin, B., Chen, J., & Zhang, X. (2015). The morphology control of hydroxyapatite microsphere at high pH values by hydrothermal method. *Advanced Powder Technology*, *26*(4), 1041–1046. https://doi.org/10.1016/j.apt.2015.04.008

Ralston, S. H. (2013). Bone structure and metabolism. *Medicine (United Kingdom)*, *41*(10), 581–585. https://doi.org/10.1016/j.mpmed.2013.07.007

Ramesh, S. (2007). Properties of hydroxyapatite produced by annealing of bovine bone, *33*, 1171–1177. https://doi.org/10.1016/j.ceramint.2006.04.001

Ramesh, S., Aw, K. L., Tolouei, R., Amiriyan, M., Tan, C. Y., Hamdi, M., … Teng, W. D. (2013). Sintering properties of hydroxyapatite powders prepared using different methods. *Ceramics International*, *39*(1), 111–119. https://doi.org/10.1016/j.ceramint.2012.05.103

Rocha-Rangel, E. (2011). Fracture Toughness Determinations by Means of Indentation Fracture. *Nanocomposites with Unique Properties and Applications in Medicine and Industry,* (c). https://doi.org/10.5772/18127

Rujitanapanich, S., Kumpapan, P., & Wanjanoi, P. (2014). Synthesis of Hydroxyapatite from Oyster Shell via Precipitation. *Energy Procedia*, *56,* 112–117. https://doi.org/10.1016/j.egypro.2014.07.138

Sadat-shojai, M., Khorasani, M., Dinpanah-khoshdargi, E., & Jamshidi, A. (2013). Acta Biomaterialia Synthesis methods for nanosized hydroxyapatite with diverse structures. *Acta Biomaterialia,* *9*(8), 7591–7621. https://doi.org/10.1016/j.actbio.2013.04.012

Seok, D., Hong, K., Young, S., & Kook, J. (2012). Processing Research Fabrication of hydroxyapatite bioceramics from the recycling of pig bone, *13*(5), 586–589.

Sheikh, F. A., & Yong, H. (2008). Extraction of pure natural hydroxyapatite from the bovine bones bio waste by three different methods, *9*, 3408–3415. https://doi.org/10.1016/j.jmatprotec.2008.07.040

Szcze, A., Ho, L., & Chibowski, E. (2017). Synthesis of hydroxyapatite for biomedical applications, *249*(April), 321–330. https://doi.org/10.1016/j.cis.2017.04.007

Tsuzuki, T. (2003). Mechanochemical Synthesis of Nanoparticles. *European Science Editing*, *38*(2), 35–37. https://doi.org/10.1023/B

Ulfyana, D., Anugroho, F., Azis, Y., Adrian, M., Deb, P., Deoghare, A. B., & Barua, E. (2017). Synthesis of Hydroxyapatite through Ultrasound and Calcination Techniques Synthesis of Hydroxyapatite through Ultrasound and Calcination Techniques.

Venkatesan. (2015). Isolation and characterization of nano-hydroxyapatite from salmon fish bone. *Materials*, *8*(8), 5426–5439. https://doi.org/10.3390/ma8085253

Venkatesan, J. (2013). Hydroxyapatite from Marine Fish Bone, (October 2016). https://doi.org/10.1201/b14723-4

Venkatesan, J., Qian, Z. J., & Ryu, B. (2011). A comparative study of thermal calcination and an alkaline hydrolysis method in the isolation of hydroxyapatite from Thunnus obesus bone. https://doi.org/10.1088/1748-6041/6/3/035003